

# COMBINATORIAL MODEL FOR THE CLUSTER CATEGORIES OF TYPE E

LISA LAMBERTI

ABSTRACT. In this paper we give a geometric-combinatorial description of the cluster categories of type  $E$ . In particular, we give an explicit geometric description of all cluster tilting objects in the cluster category of type  $E_6$ . The model we propose here arises from combining two polygons, and it generalises the description of the cluster category of type  $A$  and  $D$ .

## 1. INTRODUCTION

Caldero-Chapoton-Schiffler defined in [5] categories arising from homotopy classes of paths between two vertices of a regular  $(n+3)$ -sided polygon. Independently, Buan-Marsh-Reiten-Reineke-Todorov defined cluster categories as certain orbit categories of the bounded derived category of hereditary algebras, see [3]. The latter are algebras arising from oriented graphs  $Q$  with no oriented cycles. When  $Q$  is an orientation of a Dynkin graph of type  $A_n$ , the category constructed in [5] coincides with the one of [3]. In this paper we model a number of different orbit categories arising from orientations of tree graphs  $T_{r,s,t}$  in geometric terms. The description we propose here is based on the idea of doubling the set of oriented diagonals in a given regular polygon and combine the dynamics of these two sets in an appropriate way.

Among the additive categories we can model in this way we find cluster categories of type  $T_{r,s,t}$ , as well as other triangulated categories of various Calabi-Yau dimension. All these categories arise as mesh categories of a translation quiver whose vertices are single coloured oriented and paired diagonals in a polygon  $\Pi$ . We will see that polygons of different sizes yield different categories and these are Calabi-Yau of dimension two only in few exceptional cases. The advantage of our approach is that we can model the combinatorics of these various categories in terms of configurations of diagonals in  $\Pi$ .

For a tree diagram  $T_{r,s,t}$  let  $\mathcal{C}_{T_{r,s,t}}$  be cluster category of type  $T_{r,s,t}$  defined as the orbit category  $\mathcal{D}^b(\text{mod } kT_{r,s,t})/\tau^{-1}\Sigma$ . Then for  $n \geq \max\{r+t+1, r+s+1\}$  and a regular  $(n+3)$ -gon  $\Pi$ , we construct an additive category  $\mathcal{C}_{r,s,t}^{n+3}$  of coloured oriented single and paired diagonals of  $\Pi$ .

With this notation our first main result can be stated as follows.

**Theorem (4.3).** *We have the following equivalences of additive categories:*

$$\begin{aligned}\mathcal{C}_{1,2,2}^7 &\rightarrow \mathcal{C}_{E_6} \\ \mathcal{C}_{1,2,3}^{10} &\rightarrow \mathcal{C}_{E_7} \\ \mathcal{C}_{1,2,4}^{16} &\rightarrow \mathcal{C}_{E_8}.\end{aligned}$$

When  $T_{r,s,t}$  is not of Dynkin type we obtain an equivalence from the category  $\mathcal{C}_{r,s,t}^\infty$  associated to the infinite sided-polygon  $\Pi^\infty$  to the full subcategory of the cluster category  $\mathcal{C}_{T_{r,s,t}}$  with indecomposable objects in the transjective component of the AR-quiver of  $\mathcal{C}_{T_{r,s,t}}$ .

These equivalences enable us to investigate the combinatorics of the cluster category in geometric terms. More precisely, we are able to describe all 833 cluster tilting sets of the cluster category of type  $E_6$ ,  $\mathcal{C}_{E_6}$ , as cluster configuration of six single coloured oriented and paired diagonals in a heptagon. The strategy will be to first determine two fundamental families of cluster configurations  $\mathcal{F}_1$  and  $\mathcal{F}_2$  and deduce the remaining cluster tilting sets using the rotation inside  $\Pi$ , induced from the Auslander-Reiten translation  $\tau$  in  $\mathcal{C}_{E_6}$ , as well as a symmetry  $\sigma$  of our model.

**Theorem (5.10).** *In a heptagon*

- 350 different cluster configurations have one long paired diagonal, and they arise from  $\mathcal{F}_1$  through  $\tau$ .
- 483 other cluster configurations arise from  $\mathcal{F}_2$  through  $\sigma$  and  $\tau$ .

This classification allows us to deduce the following result.

**Theorem (5.12).** *All 833 cluster tilting sets of  $\mathcal{C}_{E_6}$  can be expressed as configurations of six non-crossing coloured oriented single and paired diagonals inside two heptagons.*

The previous results enable us to deduce geometrical moves describing the mutation process between cluster tilting objects in  $\mathcal{C}_{E_6}$ . The geometrical moves we find extend the mutation process of cluster categories of type  $A_n$ , as described by Caldero-Chapoton-Schiffler in [5], to the setting of coloured oriented diagonals. We will see that in many cases mutations inside  $\mathcal{C}_{E_6}$  correspond to flips of coloured oriented diagonals in  $\Pi$ . In the final part of the paper we use the previous results to categorify geometrically cluster algebras of type  $F_4$ . We also provide a geometric description of the mutation rule.

**Relation to previous work:** Geometrical models for cluster categories of other types have been investigated also in [19, 2, 21]. Moreover,

with an appropriate pairing of coloured oriented single and paired diagonals in an even sided polygon we recover the categorified geometric realisation of cluster algebras of type  $D$  given by Fomin-Zelevinsky in [9].

The number of clusters in a cluster algebra of finite type was first computed in [9]. Under the bijection of [3] one deduces the number of cluster tilting sets in the corresponding cluster categories. An explicit complete description of the cluster-tilting objects in the cluster category of type  $E_6$  and  $F_4$  however is new.

In addition, Fomin-Pylyavskyy used in [8] polygons to describe the cluster algebra structure in certain rings of  $\mathrm{SL}(V)$ -invariants. More precisely, they construct invariants determined by tensor graphs associated to diagonals of polygons. Using a heptagon, Fomin-Pylyavskyy also model the cluster algebra structure of the homogeneous coordinate ring  $\mathbb{C}[Gr_{3,7}]$  of the affine cone over the Grassmannian  $Gr_{3,7}$  of three dimensional subspaces in a seven dimensional complex vector space. By a result of Scott, [20], it is known that the ring  $\mathbb{C}[Gr_{3,7}]$  is a cluster algebra type of  $E_6$ . The approach of [8] however is different then the one we propose here, as it relies on relations satisfied by tensor graphs, called skein relations of tensor graphs.

**Organisation of the article:** In Section 2, we state some preliminary results and definitions. In particular, we state the fundamental properties of orbit categories and we remind the action of the shift functor on the Auslander-Reiten quiver of  $\mathcal{D}^b(\mathrm{mod}kQ)$ , for  $Q$  an orientation of a simply laced Dynkin diagram.

In Section 3, we construct the additive category  $\mathcal{C}_{r,s,t}^{n+3}$  associated to a regular  $(n+3)$ -gon  $\Pi$ , where  $n = \max\{r + t + 1, r + s + 1\}$ . The objects of  $\mathcal{C}_{r,s,t}^{n+3}$  will be single coloured oriented and paired diagonals of  $\Pi$ . The morphism spaces are generated by minimal rotations in  $\Pi$ , modulo certain equivalence relations.

In Section 4 we prove the equivalences of additive categories stated in Theorem 4.3. Further equivalence of additive categories will also be discussed. In Proposition 4.8 we show that there is an equivalence between the category  $\mathcal{C}_{r,s,t}^\infty$  associated to an infinite sided polygon and the full subcategory of the cluster category  $\mathcal{C}_{T_{r,s,t}}$ , whose indecomposable objects belong to the transjective component of the AR-quiver of  $\mathcal{C}_{T_{r,s,t}}$ .

In Section 5, we describe the combinatorics of  $\mathcal{C}_{E_6}$  geometrically inside a heptagon  $\Pi$ . In Theorem 5.10 and Theorem 5.12 we describe all cluster tilting sets of  $\mathcal{C}_{E_6}$  in terms of cluster configurations of coloured oriented diagonals of  $\Pi$ . In Proposition 5.3 we also describe all Ext-spaces of  $\mathcal{C}_{E_6}$  using curves of coloured oriented diagonals of  $\Pi$ . Finally,

results concerning the mutation process of cluster configurations will be stated, see Proposition 5.15.

In Section 6 we point out further applications of our work. In particular we deduce a geometric additive categorification of cluster algebras of type  $F_4$ . Moreover, we describe how our construction can be used to understand cluster tilting sets inside the cluster categories of type  $E_7$  and  $E_8$ , as well as cluster tilting sets in the transjective component of the AR-quiver of cluster categories associated to more general tree diagrams  $T_{r,s,t}$ .

## 2. PRELIMINARIES

Let  $k$  be an algebraically closed field and let  $Q$  be an acyclic quiver. Let  $\text{mod}kQ$  be the abelian category of  $k$ -finite dimensional right-modules over the path algebra  $kQ$ . Let  $\mathcal{D} := \mathcal{D}_Q := \mathcal{D}^b(\text{mod}kQ)$  be the bounded derived category of  $\text{mod}kQ$  endowed with the shift functor  $\Sigma : \mathcal{D} \rightarrow \mathcal{D}$  and the *Auslander-Reiten translation*  $\tau : \mathcal{D} \rightarrow \mathcal{D}$  characterised by  $\text{Hom}_{\mathcal{D}}(X, -)^* \cong \text{Hom}_{\mathcal{D}}(-, \Sigma\tau X)$ , for all  $X \in \mathcal{D}$ .

**2.1. Orbit categories of  $\mathcal{D}$ .** We are interested in the orbit categories  $\mathcal{C}_Q^p$  of  $\mathcal{D}$ ,  $p \in \mathbb{N}$ , generated by the action of cyclic group generated by the auto-equivalences  $F^p := (\tau^{-1}\Sigma)^p = \tau^{-p}\Sigma^p$ . The objects of  $\mathcal{C}_Q^p$  are the same as the objects of  $\mathcal{D}$  and

$$\text{Hom}_{\mathcal{C}_Q^p}(X, Y) := \bigoplus_{t \in \mathbb{Z}} \text{Hom}_{\mathcal{D}}(X, (F^p)^t Y).$$

Morphisms are composed in a natural way.

When  $p = 1$ ,  $\mathcal{C}_Q := \mathcal{C}_Q^1$  is the *cluster category of type  $Q$*  defined in [3], and independently in [5] in geometric terms for  $Q$  of type  $A_n$ . In all other cases  $\mathcal{C}_Q^p$  is the  *$p$ -repetitive cluster category* studied by the author in [15] for  $Q$  of type  $A_n$ , and introduced by Zhu in [22] for  $Q$  an acyclic quiver.

**2.2. Fundamental properties of orbit categories.** Like  $\mathcal{D}$ , the categories  $\mathcal{C}_Q^p$  are Krull-Schmidt and have finite dimensional Hom-spaces. The categories  $\mathcal{C}_Q^p$  are triangulated categories, and the projection functor  $\pi_i : \mathcal{D} \rightarrow \mathcal{C}_Q^p$ ,  $i \in \mathbb{N}$  is a triangle functor, see [13, Theorem 1]. The induced shift functor is again denoted by  $\Sigma$ . Moreover, the categories  $\mathcal{C}_Q^p$  have AR-triangles and the AR-translation  $\tau$  is induced from  $\mathcal{D}$ . The categories  $\mathcal{C}_Q^p$  also have the Calabi-Yau property, i.e.  $(\tau\Sigma)^m \xrightarrow{\sim} \Sigma^n$  as triangle functors, here we identify  $\tau\Sigma$  with the Serre functor of  $\mathcal{C}_Q^p$ . In particular, in  $\mathcal{C}_Q$  we have that  $n = 2$  and  $m = 1$ , hence  $\mathcal{C}_Q$  is Calabi-Yau of dimension 2. In  $\mathcal{C}_Q^p$  we have that  $m = 2$  and  $n = p$  in the above

isomorphism of triangle functors, thus  $\mathcal{C}_Q^p$  is said to be a Calabi-Yau category of fractional dimension  $\frac{p}{2}$ . Notice that a Calabi-Yau category of fractional dimension  $\frac{p}{2}$  is in general not a Calabi-Yau category of dimension 2. In this paper  $p \in \{1, 2\}$ , moreover we adopt the convention  $\text{Ext}_{\mathcal{C}_Q^p}^i(X, Y) := \text{Hom}_{\mathcal{C}_Q^p}(X, \Sigma^i Y)$ .

**2.3. Auslander-Reiten quiver of a Krull-Schmidt category.** A *stable translation quiver*  $(\Gamma, \tau)$  in the sense of Riedtmann, [18], is a quiver  $\Gamma$  without loops nor multiple edges, together with a bijective map  $\tau : \Gamma \rightarrow \Gamma$  called *translation* such that for all vertices  $x$  in  $\Gamma$  the set of starting points of arrows which end in  $x$  is equal to the set of end points of arrows which start at  $\tau(x)$ .

For  $(\Gamma, \tau)$  one defines the mesh category as the quotient category of the additive path category of  $\Gamma$  by the mesh ideal, see for example [14]. In particular, the mesh category of  $(\Gamma, \tau)$  is an additive category.

In the next result, let  $\mathbb{Z}Q$  be the repetitive quiver of  $Q$ , see [11, I,5.6] for a reminder on this construction. Let  $\tau : \mathbb{Z}Q \rightarrow \mathbb{Z}Q$  be the automorphism defined on the vertices  $(n, i)$  of  $\mathbb{Z}Q$  by  $\tau(n, i) = (n-1, i)$ , for  $n \in \mathbb{Z}$ ,  $i$  a vertex of  $Q$ .

**Theorem 2.1.** [11, I,5.5] *Let  $kQ$  be a finite dimensional hereditary  $k$ -algebra. If  $Q$  is an orientation of*

- *a simply laced Dynkin graph,  $\text{AR}(\mathcal{D}^b(\text{mod } kQ))$  is isomorphic (as stable translation quiver) to  $\mathbb{Z}Q$ .*
- *an affine graph,  $\text{AR}(\mathcal{D}^b(\text{mod } kQ))$  splits into components of the form  $\mathbb{Z}Q$  and  $\mathbb{Z}A_\infty/r$ , for some  $r \in \mathbb{N}$ .*
- *a wild graph, the components of  $\text{AR}(\mathcal{D}^b(\text{mod } kQ))$  are of the form  $\mathbb{Z}Q$  and  $\mathbb{Z}A_\infty$ .*

Let  $\text{ind } \mathcal{D}$  be the full subcategory of  $\mathcal{D}$  of indecomposable objects.

**Theorem 2.2.** [11, I,5.6] *Let  $Q$  be an orientation of a simply laced Dynkin graph. The mesh category of  $(\mathbb{Z}Q, \tau)$  is equivalent to  $\text{ind } \mathcal{D}$ .*

A first important consequence of this result is that the AR-quiver of  $\mathcal{D}$  is independent of the orientation of  $Q$ .

**2.4. Induced action of  $\Sigma$  on  $\mathbb{Z}Q$ .** In this section let  $Q$  be an orientation of a simply-laced Dynkin graph. Below we point out some known facts about the induced action of  $\Sigma$  and  $\tau$  on  $\mathbb{Z}Q$  taken from [17, Chap. 4], see also [12, Chap. 4]. These considerations, together with Theorem 2.1, will enable us to determine the precise shape of the AR-quiver of various orbit categories investigated in the sequel.

The induced action of  $\tau$  on  $\mathbb{Z}Q$  is always an horizontal shift to the left. The induced action of  $\Sigma$  on  $\mathbb{Z}A_n$  coincides with a shift of  $\frac{n+1}{2}$  units

to the right, composed with a reflection along the horizontal central line of  $\mathbb{Z}A_n$ . On  $\mathbb{Z}D_n$  the action of  $\Sigma$  agrees with  $\tau^{-(n-1)}$  composed with an order two automorphism  $\rho$  defined on  $\mathbb{Z}D_n$  when  $n$  is odd. While on  $\mathbb{Z}E_6$  the action of  $\Sigma$  coincides with the action of  $\rho\tau^{-6}$  where  $\rho$  is an automorphism of order two defined on  $\mathbb{Z}E_6$ . Moreover,  $\Sigma$  acts as  $\tau^{-9}$  on  $\mathbb{Z}E_7$ , and as  $\tau^{-15}$  on  $\mathbb{Z}E_8$ .

**2.5. The repetitive cluster category  $\mathcal{C}_{A_n}^p$ .** The geometrical model for the cluster categories of type  $E$  we propose in this paper is motivated from the following idea: glue together two copies of AR-quiver of  $\mathcal{C}_{A_n}^2$ . Let us remind the reader some facts about this category.

The previous discussion implies that  $(AR(\mathcal{C}_{A_n}^p), \tau) \cong (\mathbb{Z}A_n/(\tau^{-1}\Sigma)^p, \tau)$ , for  $p \in \mathbb{N}$ . Moreover,  $(AR(\mathcal{C}_{A_n}^p), \tau)$  can be modelled using diagonals in polygons as done in [15]. When  $p = 2$ , the quiver  $(AR(\mathcal{C}_{A_n}^2), \tau)$  can entirely be modelled using oriented diagonals in a regular  $(n+3)$ -gon. In Figure 1 an illustration of this construction is provided for  $p = 2, n = 4$ .

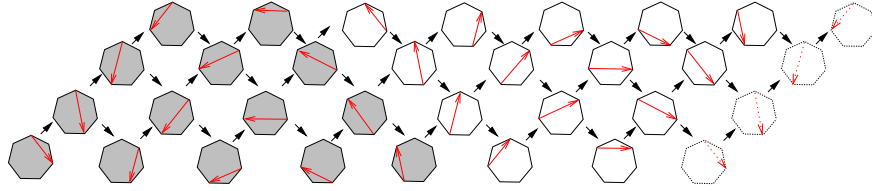


FIGURE 1. AR-quiver of  $\mathcal{C}_{A_4}^2$ .

### 3. SINGLE COLOURED ORIENTED AND PAIRED DIAGONALS IN POLYGONS

Throughout the rest of the paper let  $T_{r,s,t}$  be an orientation of a finite connected graph with  $r + s + t + 1$  vertices and three legs. We assume the legs of  $T_{r,s,t}$  to have  $r$ , resp.  $s$ , resp.  $t$  vertices and that one vertex of  $T_{r,s,t}$  has three neighbours. We say that a tree  $T_{r,s,t}$  is *symmetric* if  $s = t$ .

Unless specified otherwise, for  $n \geq \max\{r + s + 1; r + t + 1\}$  let  $\Pi$  be a regular  $(n+3)$ -gon with vertices numbered in the clockwise order by the group  $\mathbb{Z}/(n+3)\mathbb{Z}$ .

For vertices  $i, j, k$  of  $\Pi$  we write  $i \leq j \leq k$  if  $j$  is between  $i$  and  $k$  in the clockwise order. Moreover, we denote by  $(i, j)$  the unoriented diagonal of  $\Pi$  joining the vertices  $i$  and  $j$  and by  $[i, j]$  the oriented diagonal of  $\Pi$  starting at  $i$  and ending in  $j$ . We do not consider boundary segments as oriented diagonals.

**3.1. Single coloured oriented and paired diagonals of  $\Pi$ .** We start describing the geometric construction leading to the modelling of a number of orbit categories of  $\mathcal{D}^b(\text{mod } kT_{r,s,t})$  arising from orientations of symmetric trees  $T_{r,s,t}$ .

To begin the construction we double the set of oriented diagonals of  $\Pi$ , and distinguish each set with colours using subscripts  $R, B$  e.g.  $[1, 3]_R$  is the red diagonal linking the vertex 1 to 3 of  $\Pi$ . For every vertex  $i$  of  $\Pi$  we form the following  $(r + 1)$  pairs of coloured oriented diagonals:

$$\begin{aligned} [i, i + 2]_P = [i + 2, i]_P &:= \{[i, i + 2]_R, [i + 2, i]_B\} \\ [i, i + 3]_P = [i + 3, i]_P &:= \{[i, i + 3]_R, [i + 3, i]_B\} \\ &\dots \\ [i, i + r + 2]_P = [i + r + 2, i]_P &:= \{[i, i + r + 2]_R, [i + r + 2, i]_B\}. \end{aligned}$$

When  $r = 0$ , we assume that there are no paired diagonals. Moreover, let us point out that  $[i, j]_P \neq [j, i]_P$ .

Next we define a subset of  $(r + 1)(n + 3)$  paired,  $s(n + 3)$  single red and  $t(n + 3)$  single blue oriented diagonals of  $\Pi$  as follows:

$$\Pi_{r,s,t} := \left\{ [i, i + 2]_P, \dots, [i, i + r + 2]_P, \right. \\ \left. [i, i + r + 3]_R, \dots, [i, i + r + s + 2]_R, \right. \\ \left. [i + r + 3, i]_B, \dots, [i + r + t + 2, i]_B, \quad i \text{ vertex of } \Pi \right\}.$$

Once coloured oriented diagonals are paired, they stop existing as single coloured oriented diagonals in  $\Pi_{r,s,t}$ .

Consider the subset of elements of  $\Pi_{r,s,t}$  given by  $\Pi_{r,s,t}|_1 := \{[1, 3]_P, \dots, [1, r + 3]_P, [1, r + 4]_R, \dots, [1, r + s + 3]_R, [r + 4, 1]_B, \dots, [r + t + 3, 1]_B\}$ . Then on the one side elements of  $\Pi_{r,s,t}|_1$  are in bijection with the vertices of  $T_{r,s,t}$ . On the other side, elements of  $\Pi_{r,s,t}|_1$  give rise to a triangulation of a region inside  $\Pi$  homotopic to a regular  $(r + s + 4)$ -gon, resp. to a  $(r + t + 4)$ -gon.

In Figure 2 an illustration of this situation is provided. Coloured oriented diagonals with the same label are identified. The black vertices in the figure represent the vertices of  $T_{r,s,t}$ . The dotted lines are the edges of  $T_{r,s,t}$ . Vertices on, and edges between, identified paired diagonals give rise to one vertex, and one edge, in  $T_{r,s,t}$ .

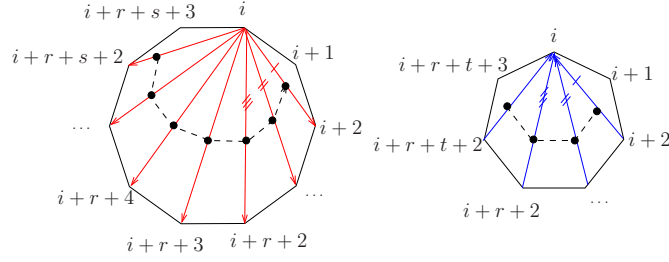


FIGURE 2. The coloured oriented diagonals in bijection with the vertices of  $T_{2,4,1}$ .

**3.2. The automorphisms  $\rho$  and  $\tau$ .** Our next aim is to define two automorphisms:  $\rho$  and  $\tau$ , acting on the set of coloured oriented single an paired diagonals of  $\Pi$  associated to a tree  $T_{r,s,t}$ . The first automorphism is induced from the graph automorphism of a symmetric tree, hence only defined on  $\Pi_{r,t,t}$ . The definition of the second automorphism depends on the parity of the number of sides of  $\Pi$ .

Let  $c \in \{R, B, P\}$ . Then we define  $\rho : \Pi_{r,t,t} \rightarrow \Pi_{r,t,t}$  as the automorphism of order two given by

$$\rho([i, j]_c) := \begin{cases} [j, i]_B & \text{if } c = R, \\ [j, i]_R & \text{if } c = B, \\ [i, j]_P & \text{otherwise.} \end{cases}$$

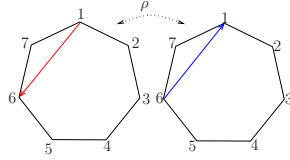


FIGURE 3. The symmetry  $\rho$ .

Moreover, we define the automorphism  $\tau : \Pi_{r,s,t} \rightarrow \Pi_{r,s,t}$  as follows: if  $s \neq t$ , then  $\tau([i, j]_c) := [i-1, j-1]_c$ . If  $s = t$ , then

$$\tau([i, j]_c) := \begin{cases} \rho^{(n+3)}([i-1, j-1]_c) & \text{if } [i, j]_c \in \Pi_{r,t,t}|_1 \\ [i-1, j-1]_c & \text{otherwise.} \end{cases}$$

Geometrically, the action of  $\tau$  is given by the anticlockwise rotation through  $\frac{2\pi}{n+3}$  around the centre of  $\Pi$ , on all elements different then the diagonals in  $\Pi_{r,t,t}|_1$  associated to a symmetric tree in a polygon with an odd number of sides. On the latter the rotation is followed by the simultaneous change of colour and orientation.

**3.3. Minimal clockwise rotations.** Minimal clockwise rotations for unoriented diagonals have been introduced in [5, §2] with the aim of modelling irreducible morphisms in the cluster category  $\mathcal{C}_A$ . Following the spirit of [5] we now define minimal rotations between diagonals of  $\Pi_{r,s,t}$ .

Let  $k, l$  be non-neighbouring vertices of  $\Pi$  and let  $c \in \{R, B, P\}$ . Let  $\Pi_{r,s,t}$  be the set of coloured oriented single and paired diagonals in  $\Pi$  associated to an asymmetric tree  $T_{r,s,t}$ . Then the following three operations between diagonals in  $\Pi_{r,s,t}$  are called *minimal clockwise rotation*:  $[k, l]_c \rightarrow [k, l + 1]_c$  and  $[k, l]_c \rightarrow [k + 1, l]_c$  and

$$\begin{array}{ccc}
 & [k, k + r + 3]_R & \\
 \nearrow & & \searrow \\
 [k, k + r + 2]_P & & [k + 1, k + r + 3]_P \\
 \searrow & & \nearrow \\
 & [k + r + 3, k]_B &
 \end{array}$$

Next, let  $\Pi_{r,t,t}$  be the set of coloured oriented single and paired diagonals in  $\Pi$  associated to a symmetric tree  $T_{r,t,t}$ . Then minimal clockwise rotations are defined as before with the following adjustment: when  $[k, l]_c, [k, k + r + 2]_P$  are in  $\tau(\Pi_{r,t,t}|_1)$  and  $\Pi$  is odd sided, then we also change simultaneously the colour and the orientation.

In Figure 4 and Figure 5 illustrations of the three minimal rotations described above can be found.

The next remark can be used to model orbit categories arising from orientations of tree graphs  $T_{r_1, r_2, \dots, r_m}$  where one vertex has  $m$  neighbours.

**Remark 3.1.** *There are three minimal rotations linking the three types of coloured oriented single and paired diagonals of  $\Pi_{r,r,t}$ , namely the red, the blue and the paired ones. Starting with oriented diagonals coloured in  $m - 1$  ways, one can describe the  $m$  minimal rotations linking the  $m$  types of coloured oriented diagonals with a similar diagram as above.*

**3.4. Quivers of single coloured oriented and paired diagonals of  $\Pi_{r,s,t}$ .** Let  $\Gamma_{r,s,t}^{n+3}$  be the quiver whose vertices are the elements of  $\Pi_{r,s,t}$ . An arrow between two vertices of  $\Gamma_{r,s,t}^{n+3}$  is drawn whenever there is a minimal clockwise rotation linking them. No arrow is drawn otherwise.

Concerning the shape of  $\Gamma_{r,s,t}^{n+3}$  we remark that  $\Gamma_{r,s,t}^{n+3}$  always lies on a cylinder, except when  $\Pi$  is odd-sided, and  $s = t$ . Then we say that  $\Gamma_{r,t,t}^{n+3}$  lies on a Möbius strip, since the  $\tau$ -orbits of single coloured oriented diagonals are twice as long as the  $\tau$ -orbits of paired diagonals.

In Figure 4 the quiver  $(\Gamma_{1,1,1}^6, \tau)$  of coloured oriented diagonals in a hexagon, as well as the quiver  $(\Gamma_{1,2,2}^7, \tau)$  associated to a heptagon are

illustrated. In each quiver we indicate in the last slice the identifications occurring. On both quivers the action of  $\tau$  is always given by a shift to the left.

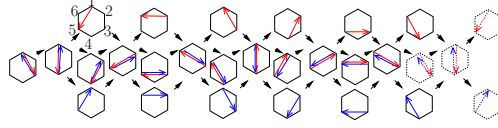


FIGURE 4. The quiver  $(\Gamma_{1,1,1}^6, \tau)$  corresponds to the AR-quiver of the orbit category  $\mathcal{D}^b(\text{mod } kD_4)/\Sigma^2$ .

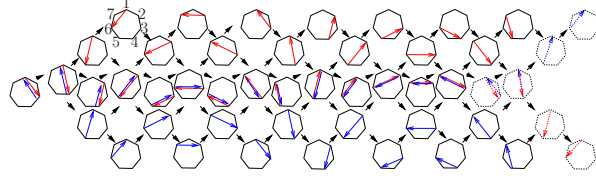


FIGURE 5. The quiver  $(\Gamma_{1,2,2}^7, \tau)$  corresponds to the AR-quiver of the orbit category  $\mathcal{D}^b(\text{mod } kE_6)/\tau^{-1}\Sigma$ .

#### 4. EQUIVALENCES OF CATEGORIES

In this section we show that the construction of  $\Gamma_{r,s,t}^{n+3}$  and  $\Gamma_{r,s,t}^{n+3}$  allow us to model geometrically properties of a number of additive categories.

Let  $\rho$  be the automorphism of  $T_{r,t,t}$  and let  $n \geq \max\{r+t+1, r+s+1\}$ . Then we can show the following opening result.

**Lemma 4.1.** *The quiver  $(\Gamma_{r,s,t}^{n+3}, \tau)$  is a stable translation quiver.*

*Proof.* We have to show three things. First, that  $\Gamma_{r,s,t}^{n+3}$  is connected, has no loops, and is locally finite. Second, that for every vertex  $v$  of  $\Gamma_{r,s,t}^{n+3}$  the number of arrows going to  $v$  equals the number of arrows leaving  $v$ . Third, that the map  $\tau$  is bijective.

All the above properties follow from the construction. Let us first consider the symmetric case. Then it is not hard to see that when  $\Pi$  is even sided,  $\Gamma_{r,t,t}^{n+3}|_R \cong \mathbb{Z}A_{r+t+1}/\tau^{-(n+3)}$  and  $\Gamma_{r,t,t}^{n+3}|_B \cong \mathbb{Z}A_{r+t+1}/\tau^{-(n+3)}$  since we consider oriented arcs. Thus, we deduce that  $(\Gamma_{r,t,t}^{n+3}|_R, \tau|_R)$  and  $(\Gamma_{r,t,t}^{n+3}|_B, \tau|_B)$  are stable translation quivers. Forming pairs of coloured oriented diagonals results in gluing these two quivers along  $r$  disjoint  $\tau$ -orbits, and the above properties are preserved. When  $\Pi$  is odd sided one can check that the modifications in the definition of minimal clockwise rotations and in the definition of  $\tau$  are such that the resulting quiver has the claimed properties.

Finally, it is not hard to see that also  $\Gamma_{r,s,t}^{n+3}$  associated to an asymmetric tree is a stable translation quiver.  $\square$

**Theorem 4.2.** *Let  $\mathcal{T}$  be an additively finite Krull-Schmidt category. Let  $\Gamma$  be a connected component of the AR-quiver of  $\mathcal{T}$ . Assume that  $\Gamma \cong \mathbb{Z}T_{r,s,t}/\tau^{-(n+3)}$ , resp.  $\Gamma \cong \mathbb{Z}T_{r,t,t}/\tau^{-(n+3)}\rho$ . Then there is an isomorphism of stable translation quivers  $\Gamma_{r,s,t}^{n+3} \rightarrow \Gamma$ , for  $\Gamma_{r,s,t}^{n+3}$  associated to a regular  $(n+3)$ -gon.*

*Proof.* The claim follows from the proof of Lemma 4.1, since we saw that the following are isomorphisms of stable translation quivers:  $\Gamma_{r,s,t}^{n+3} \xrightarrow{\cong} \mathbb{Z}T_{r,s,t}/\tau^{-(n+3)}$ ,  $\Gamma_{r,t,t}^{n+3} \xrightarrow{\cong} \mathbb{Z}T_{r,t,t}/\tau^{-(n+3)}\rho^{(n+3)}$  for all integers  $r, s, t$  and  $n$  as above.  $\square$

**4.1. Projections.** Our next goal is to define a translation quiver  $\Gamma_{r,t}^{n+3}$  obtained from  $\Gamma_{r,t,t}^{n+3}$  associated to a symmetric tree  $T_{r,t,t}$  after folding  $\Gamma_{r,t,t}^{n+3}$  along its central line.

For this consider again the graph automorphism  $\rho$  induced by the map simultaneously changing colour and orientation of the diagonals in  $\Pi_{r,t,t}$ . Then the vertices of  $\Gamma_{r,t}^{n+3}$  are the  $\rho$ -orbits of vertices of  $\Gamma_{r,t,t}^{n+3}$ , i.e. the pairs  $\{[i, i+j]_R, [i+j, i]_B\}$ , for  $i, j$  in vertices of  $\Pi$ . The arrows in  $\Gamma_{r,t}^{n+3}$  are always single and coincide with minimal clockwise rotation around a common vertex of  $\Pi$  linking pairs of coloured oriented diagonals. The translation on  $\Gamma_{r,t}^{n+3}$  is induced from the translation in  $\Gamma_{r,t,t}^{n+3}$  and given by the anti clockwise rotation through  $\frac{2\pi}{n+3}$  around the center of  $\Pi$ .

Clearly,  $\Gamma_{r,t,t}^{n+3} \rightarrow \Gamma_{r,t}^{n+3}$  is a surjective map of stable translation quivers.

**4.2. Cluster categories of type  $E_6$ ,  $E_7$  and  $E_8$ .** As a corollary of Theorem 4.2 we obtain the geometrical modelling of cluster categories  $\mathcal{C}_{T_{r,s,t}}$  where  $T_{r,s,t}$  is an arbitrary tree. Since the number of connected components of the AR-quiver of  $\mathcal{C}_{T_{r,t,t}}$  varies with the shape of  $T_{r,t,t}$ , we proceed considering two cases. In this section we focus on tree graphs of Dynkin type, in Section 4.4 the general case will be treated.

In view of Theorem 4.3 below let  $\mathcal{C}_{r,s,t}^{n+3}$  be the additive category generated by the mesh category of  $\Gamma_{r,s,t}^{n+3}$ , for  $r, s, t, n \in \mathbb{N}$ . Then we can show the main result of this section.

**Theorem 4.3.** *We have the following equivalences of additive categories*

$$\begin{aligned}\mathcal{C}_{1,2,2}^7 &\rightarrow \mathcal{C}_{E_6} \\ \mathcal{C}_{1,2,3}^{10} &\rightarrow \mathcal{C}_{E_7} \\ \mathcal{C}_{1,2,4}^{16} &\rightarrow \mathcal{C}_{E_8}.\end{aligned}$$

*Proof.* Since the full subcategories of indecomposable objects of the orbit categories we consider are equivalent to the mesh category of their AR-quiver, we only have to check that there is an isomorphism of stable translation quivers between the AR-quiver of the various orbit categories and the quivers of coloured oriented single and paired diagonals associated to  $\Pi$ . This isomorphism then induces the claimed equivalences.

To do so, the strategy will be to compare the action of  $\tau$  on  $\Gamma_{r,s,t}^{n+3}$  with the actions of  $\tau$  and of  $\Sigma$  on  $\mathbb{Z}Q$  where  $Q$  is an orientation of a simply laced Dynkin diagram, as described in Section 2.4.

Below we treat the case  $\mathcal{C}_{E_7}$ , the remaining two claims can be deduced with a similar reasoning. From the discussion of Section 2.4 it follows that the AR-quiver of  $\mathcal{C}_{E_7}$  is isomorphic to the quotient graph  $\mathbb{Z}E_7/\tau^{-10}$ . On the other side, by definition  $\mathcal{C}_{1,5,5}^{10}$  is the mesh category of  $\Gamma_{1,5,5}^{10}$  associated to a 10-gon and  $\Gamma_{1,5,5}^{10} \cong \mathbb{Z}E_7/(\tau^{-10}) \cong \tau^{-1}\Sigma$ .  $\square$

**Corollary 4.4.** *We also deduce the following equivalences of additive categories*

$$\begin{aligned}\mathcal{C}_{r,0,0}^{r+4} &\rightarrow \mathcal{C}_{A_{r+1}}^2 \\ \mathcal{C}_{r,s,0}^{r+s+4} &\rightarrow \mathcal{C}_{A_{r+s+1}}^2 \\ \mathcal{C}_{r,0,t}^{r+t+4} &\rightarrow \mathcal{C}_{A_{r+t+1}}^2 \\ \mathcal{C}_{r,1,1}^{r+5} &\rightarrow \mathcal{D}^b(\text{mod}D_{r+3})/\tau^{-3}\Sigma.\end{aligned}$$

*Proof.* We follow the proof of Theorem 4.3 and observe that for the first claim we consider only paired oriented diagonals of  $\Pi$ . Since  $[i, j]_P \neq [j, i]_P$  and the map  $\rho$  is the identity on paired oriented diagonals, we deduce that  $\Gamma_{r,0,0}^{r+4}$  always lies on a cylinder. From Lemma 4.1 we deduce that  $\Gamma_{r,0,0}^{r+4} \cong \mathbb{Z}A_{r+1}/\tau^{-(r+3)}$ . From the discussion of Section 2.4 we deduce that  $\mathbb{Z}A_{r+1}/\tau^{-(r+3)} \cong \mathbb{Z}A_{r+1}/\tau^{-2}\Sigma$  which we recognise as the AR-quiver of  $\mathcal{D}^b(\text{mod}kA_{r+1})/\tau^{-2}\Sigma^2$ .

The second and third claim follow in a similar fashion.

For the last claim we observe that for each vertex of  $\Pi$  the quiver  $\Gamma_{r,1,1}^{r+5}$  has one red and one blue single coloured oriented diagonal. These

correspond to the exceptional vertices of a Dynkin diagram of type  $D_{r+3}$ .  $\square$

**Remark 4.5.** *The equivalences of Theorem 4.3 and Corollary 4.4 allow us to define a shift functor  $\Sigma$  on the categories associated to  $\Pi$  induced by the shift functor  $\Sigma$  defined on the various orbit categories considered above, see also [16]. In the following however, we will not use the triangulated structure of these categories.*

Let  $[i, j]_c$ ,  $c \in \{R, B, P\}$ , be a coloured oriented single or paired diagonal of a heptagon  $\Pi$  and let  $(i, j)$  be the underlying unoriented diagonal. Then we deduce the following useful results.

**Corollary 4.6.** *There is a dense and full functor*

$$\begin{aligned} \mathcal{C}_{E_6} &\rightarrow \mathcal{C}_{A_4} \\ [i, j]_c &\mapsto (i, j) \end{aligned}$$

*from the cluster category  $\mathcal{C}_{E_6}$  of type  $E_6$  to the cluster category  $\mathcal{C}_{A_4}$  of type  $A_4$ .*

*Proof.* Consider the projection  $\pi_1 : \Gamma_{1,2,2}^7 \rightarrow \Gamma_{1,2}^7$  defined in Subsection 4.1. Let  $\Gamma$  be the stable translation quiver of unoriented diagonals of  $\Pi$ , as defined in Caldero-Chapoton-Schiffler's paper [5]. Then there is a projection  $\pi_2 : \Gamma_{1,2}^7 \rightarrow \Gamma$ , which maps  $\{[i, i+j]_R, [i+j, i]_B\}$  to the unoriented diagonal  $(i, i+j)$  of  $\Pi$  and pairs of arrows in  $\Gamma_{1,2}^7$  to the one corresponding arrow in  $\Gamma$ . We get a surjective map of translation quivers  $\pi_2 \circ \pi_1 : \Gamma_{1,2,2}^7 \rightarrow \Gamma$ . This map then induces a dense and full functor

$$\mathcal{C}_{E_6} \rightarrow \mathcal{C}_{A_4},$$

after identifying  $\mathcal{C}_{E_6}$ , resp.  $\mathcal{C}_{A_4}$ , with the additive category generated by the mesh category of  $\Gamma_{1,2,2}^7$ , resp.  $\Gamma$ .  $\square$

In Section 5 we will use the functor  $\mathcal{C}_{E_6} \rightarrow \mathcal{C}_{A_4}$  to describe all cluster tilting sets of  $\mathcal{C}_{E_6}$  as configurations of coloured oriented diagonals in  $\Pi$ .

**Corollary 4.7.** *There is a dense and full functor*

$$\begin{aligned} \mathcal{C}_{r,0,0}^{r+4} &\rightarrow \mathcal{C}_{A_{r+1}} \\ [i, j]_P &\mapsto (i, j) \end{aligned}$$

*from the category  $\mathcal{C}_{r,0,0}^{r+4}$  to the cluster category of type  $A_{r+1}$ .*

*Proof.* Follows from the proof of Corollary 4.4.  $\square$

**4.3. Coloured oriented single and paired diagonals and the cluster category of type  $D_n$ .** The aim of this section is to link our category of coloured oriented single and paired diagonals to the cluster category of type  $D_n$ , denoted by  $\mathcal{C}_{D_n}$ . We recall that  $\mathcal{C}_{D_n}$  can be modelled geometrically in two equivalent ways. One approach arises categorifying the model given by Fomin-Zelevinsky in [9, Prop. 3.16] defined in terms of unoriented diameters and pairs of diagonals in a regular  $2n$ -gon. The second approach uses tagged arcs in a once punctured disc, as described by Schiffler in [19]. We can recover both descriptions from our model.

For the first one, we proceed as follows. Let  $(\Gamma_{n-3,n-1,n-1}^{2n}, \tau)$  be as before and define the quiver  $\Gamma_{D_n}$  having as vertices the (unordered) triples of centrally symmetric diagonals of  $\Pi$ :

$$\begin{aligned} & \{[i, i+2]_P, [i+2+n, i+n]_R, [i+n, i+2+n]_B\}, \\ & \{[i, i+3]_P, [i+3+n, i+n]_R, [i+n, i+3+n]_B\}, \\ & \dots \\ & \{[i, i+n-1]_P, [i+2n-1, i+n]_R, [i+n, i+2n-1]_B\} \end{aligned}$$

together with the oriented single diagonals  $[i, n+i]_R, [n+1, i]_B$  of  $\Pi$ , for  $1 \leq i \leq 2n$ . Notice that  $[i, n+i]_R$  and  $[n+1, i]_B$  are the central oriented diagonals of  $\Pi$ . The arrows of  $\Gamma_{D_n}$  are induced by the minimal clockwise rotations between diagonals of  $\Pi_{n-3,n-1,n-1}$ , similarly for the translation map. This allows us to obtain a surjective map of stable translation quivers  $\Gamma_{n-3,n-1,n-1}^{2n} \rightarrow \Gamma_{D_n}$ . Dropping the orientations of all coloured diagonals we also obtain the surjective map  $\Gamma_{D_n} \rightarrow AR(\mathcal{C}_{D_n})$ . It follows that there is a dense and full functor

$$\mathcal{C}_{n-3,n-1,n-1}^{2n} \rightarrow \mathcal{C}_{D_n}$$

from the mesh category of  $\Gamma_{n-3,n-1,n-1}^{2n}$ ,  $\mathcal{C}_{n-3,n-1,n-1}^{2n}$ , to the cluster category  $\mathcal{C}_{D_n}$ . In addition, we observe that  $\Gamma_{D_n} \cong \mathbb{Z}D_n/(\tau^{-1}\Sigma)^2 \cong AR(\mathcal{C}_{D_n}^2)$ , where  $\mathcal{C}_{D_n}^2$  is the 2-repetitive cluster category of type  $D_n$  defined in Section 2.1.

To recover Schiffler's model we need to use a smaller punctured polygon and allow non-contractible loops. Defining  $\Gamma_{n-3,1,1}^n$  and  $\mathcal{C}_{n-3,1,1}^n$  as before we obtain an isomorphism of stable translation quivers  $\Gamma_{n-3,1,1}^n \xrightarrow{\cong} AR(\mathcal{C}_{D_n})$  and the desired equivalence of categories:  $\mathcal{C}_{n-3,1,1}^n \xrightarrow{\cong} \mathcal{C}_{D_n}$ . In Figure 6 we illustrate the quiver  $\Gamma_{1,1,1}^4$  in a regular punctured square.

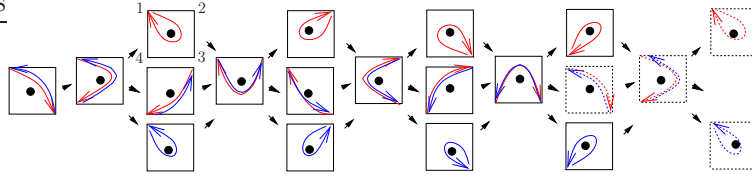


FIGURE 6. The quiver  $\Gamma_{1,1,1}^4 \cong AR(\mathcal{C}_{D_4})$  in a square.

#### 4.4. Cluster categories associated to trees not of Dynkin type.

When  $T_{r,s,t}$  is not an orientation of a simply laced Dynkin graph the AR-quiver of the cluster category  $\mathcal{C}_{T_{r,s,t}}$  splits into various connected components. Our next goal is to obtain an isomorphism between the irregular (transjective) component of the AR-quiver of  $\mathcal{C}_{T_{r,s,t}}$  and the quiver of coloured oriented single and paired diagonals.

For this we extend the construction of Section 3.1 and consider an infinite-sided polygon  $\Pi^\infty$ . Next, let  $\Pi_{r,s,t}^\infty$  be the subset of all coloured oriented single and paired diagonals of  $\Pi^\infty$  consisting of  $r + 1$  paired,  $s$  red and  $t$  blue single coloured oriented diagonals for every vertex of  $\Pi^\infty$ :

$$\Pi_{r,s,t} := \left\{ \begin{aligned} &[i, i + 2]_P, \dots, [i, i + r + 2]_P, \\ &[i, i + r + 3]_R, \dots, [i, i + r + s + 2]_R, \\ &[i + r + 3, i]_B, \dots, [i + r + t + 2, i]_B, \quad i \text{ vertex of } \Pi^\infty \end{aligned} \right\}.$$

Then we extend the definition of minimal clockwise rotations of Section 3.3 to this setting. Thus we obtain a quiver  $\Gamma_{r,s,t}^\infty$  whose vertices are the elements of  $\Pi_{r,s,t}^\infty$  and where we link two vertices with an arrow when there is a minimal clockwise rotation between them. Moreover, we define  $\tau$  on the elements of  $\Pi_{r,s,t}^\infty$  as the anticlockwise rotation around the center of  $\Pi^\infty$  induced by the rotation through  $\frac{2\pi}{n+3}$  in an  $(n+3)$ -gon  $\Pi$  letting  $n \rightarrow \infty$ . In this way we turn  $(\Gamma_{r,s,t}^\infty, \tau)$  into a stable translation quiver.

To state the next result, let  $\mathcal{P}$  be the full subcategory of  $\mathcal{C}_{T_{r,s,t}}$  consisting of  $\tau$ -shifts of indecomposable projective objects in  $\mathcal{C}_{T_{r,s,t}}$ . Moreover, denote the additive category generated by the mesh category of  $(\Gamma_{r,s,t}^\infty, \tau)$  by  $\mathcal{C}_{r,s,t}^\infty$ . Then we can show the following result.

**Proposition 4.8.** *The functor*

$$\varphi : \mathcal{C}_{r,s,t}^\infty \rightarrow \mathcal{P}$$

*is an equivalence of additive categories.*

*Proof.* First we observe that  $\Gamma_{r,s,t}^\infty \cong \mathbb{Z}T_{r,s,t}$ .

Next, let  $\Pi_{r,s,t}^\infty|_1$  be the subset of  $\Pi_{r,s,t}^\infty$  consisting of the  $r + s + t + 1$  single and paired diagonals:  $\{[1, 3]_P, \dots, [1, r+3]_P, [1, r+4]_R, \dots, [1, r+s+3]_R, [r+4, 1]_B, \dots, [r+t+3, 1]_B\}$ . Then, we observe that since  $\Gamma_{r,s,t}^\infty$  is a connected stable translation quiver  $\varphi$  induces an injective map between  $\text{Hom}_{\mathcal{C}_{r,s,t}^\infty}(\tau(D_j), D_i)$ , for  $D_i, D_j \in \Pi_{r,s,t}^\infty$  and  $\text{Hom}_{\mathcal{C}_{T_{r,s,t}}} (I_j, \Sigma(P_i))$  between the indecomposable injective objects and  $\Sigma$  of the projective objects in  $\mathcal{C}_{T_{r,s,t}}$ . Thus  $\varphi$  is full. Moreover, it is not hard to see that  $\varphi$  is dense and faithful, thus  $\varphi$  is indeed an equivalence of additive categories.  $\square$

## 5. COMBINATORICS OF THE CLUSTER CATEGORY $\mathcal{C}_{E_6}$

Our next aim is to describe the combinatorics of the cluster category  $\mathcal{C}_{E_6} \cong \mathcal{C}_{1,2,2}$  inside a heptagon.

Throughout the chapter let  $\Pi$  be a regular heptagon and let  $(\Gamma, \tau) := (\Gamma_{1,2,2}^7, \tau)$ . Moreover, let  $\Gamma_\Pi$  be the stable translation quiver having as vertices the unoriented diagonals of  $\Pi$  and arrows given by minimal clockwise rotations, see [5] for details.

**5.1. Extension spaces in  $\mathcal{C}_{E_6}$ .** The support of  $\text{Hom}(\tau^{-1}X, -)$  in  $\mathcal{C}_Q$  is called the *front Ext-hammock of  $X$* . The support of  $\text{Hom}(-, \tau X)$  in  $\mathcal{C}_Q$  is called the *back Ext-hammock of  $X$* . These hammocks can be deduced from the AR-quiver using mesh relations, or using starting and ending functions, see [3, Chap. 8]. For AR-quivers isomorphic to  $\mathbb{Z}Q$  with  $Q$  an orientation of a Dynkin graph, the support of  $\text{Hom}(-, -)$  has been described in detail in [1].

Identify again  $\mathcal{C}_{E_6}$ , resp.  $\mathcal{C}_{A_4}$  with the additive categories generated by the mesh categories of  $\Gamma$ , resp.  $\Gamma_\Pi$ . In the sequel we view the hammocks inside  $\Gamma$  or  $\Gamma_\Pi$ . Moreover, let  $\text{Ext}_\Pi^1(D_X, D_Y) := \text{Ext}_{\mathcal{C}_{E_6}}^1(X, Y)$ , for coloured oriented diagonals  $D_X, D_Y$  in  $\Pi$  and indecomposable objects  $X$  and  $Y$  in  $\mathcal{C}_{E_6}$  corresponding to  $D_X$  and  $D_Y$  by the equivalence of Theorem 4.3.

**Remark 5.1.** *As  $\mathcal{C}_{E_6}$  is 2-Calabi-Yau:  $D\text{Ext}_{\mathcal{C}_{E_6}}^1(X, Y) \cong \text{Ext}_{\mathcal{C}_{E_6}}^1(X, Y)$ , for all objects  $X, Y$  in  $\mathcal{C}_{E_6}$ . Therefore, the back and front Ext-hammocks in  $\mathcal{C}_{E_6}$  coincide for all objects. On the other hand, in  $\mathcal{C}_{A_4}^2$  the back and front hammocks are disjoint, as the category is not 2-Calabi-Yau.*

**5.2. Lift of hammocks.** Consider again the projection  $\tilde{\pi} := \pi_2 \circ \pi_1 : \Gamma \rightarrow \Gamma_\Pi$  defined by  $D_{(i,j)} := \tilde{\pi}(D_X)$  as in Corollary 4.6. For each  $D_X$  we define two connected sub-quivers of  $\Gamma$ ,  $I_1(D_X)$  and  $I_2(D_X)$ , as follows. The vertices of both  $I_1(D_X)$  and  $I_2(D_X)$ , are the vertices of  $\Gamma$  in the

Ext-hammock of  $D_X$  in  $\Gamma$  and in the preimage under  $\tilde{\pi}$  of the Ext-hammock of  $D_{(i,j)}$  in  $\Gamma_\Pi$ . The arrows of  $I_1(D_X)$  and  $I_2(D_X)$  coincide with the arrows of  $\Gamma$ . Then  $I_1(D_X)$  contains the vertex  $\tau^{-1}(D_X)$  and will be called the *front crossing* of  $D_X$ ,  $I_2(D_X)$  contains  $\tau(D_X)$  and will be called the *back crossing* of  $D_X$ .

Note that for all  $D_X$ , the sub-quivers  $I_1(D_X)$  and  $I_2(D_X)$  are disjoint. In addition, all coloured oriented diagonals in  $\Pi$  crossing  $D_X$  in an interior point of  $D_X$  are vertices of  $I_1(D_X) \cup \rho(I_1(D_X))$  and  $I_2(D_X) \cup \rho(I_2(D_X))$ . See Figure 7, were the vertices of inside the front and back crossings of  $D_X$  are in heptagons with bold boundary, for  $D_X$  a coloured oriented diagonal in the first slice of  $\Gamma$ .

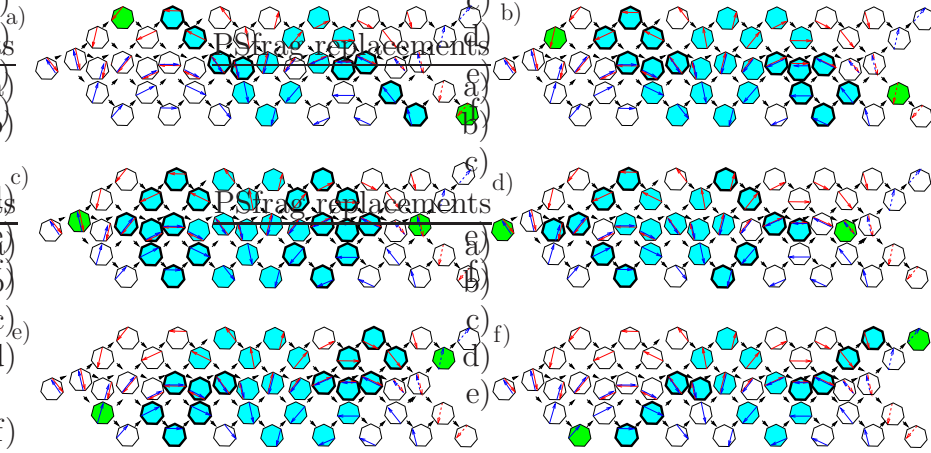


FIGURE 7. The Ext-hammocks of the diagonals with vertices of  $I_1$  and  $I_2$  represented in heptagons with bold boundary.

In the next result, we assume that  $D_X$  is a coloured oriented diagonal of  $\Pi$  in the first slice of  $\Gamma$ . This assumption can be dropped using  $\tau$ -shifts, or renumbering the vertices of  $\Pi$ . Moreover, we write  $\partial\Pi$  to indicate the boundary of  $\Pi$ , and for two coloured oriented diagonals  $D_X$  and  $D_Y$  we say that  $D_Y$  enters the smaller region bounded by  $D_X$  and  $\partial\Pi$  if the arrow head of  $D_Y$  goes to a vertex of  $\partial\Pi$  inside the region and different from the vertices joined by  $D_X$ .

**Proposition 5.2.** *Let  $D_X, D_Y$  be coloured oriented diagonals of  $\Pi$ . Assume  $D_X$  is in the first slice of  $\Gamma$ , and that  $D_X$  crosses  $D_Y$ .*

- *If  $D_X$  is a paired diagonal, then  $\dim_k(\text{Ext}_\Pi^1(D_X, D_Y)) = 1$ .*
- *If  $D_X$  is a single diagonal, and  $D_Y$  enters the smaller region bounded by  $D_X$  and  $\partial\Pi$ , then  $\dim_k(\text{Ext}_\Pi^1(D_X, D_Y)) = 1$ .*

*Proof.* If  $D_X$  is paired,  $I_1(D_X)$  coincides with  $I_1(D_X) \cup \rho(I_1(D_X))$  and  $I_2(D_X)$  coincides with  $I_2(D_X) \cup \rho(I_2(D_X))$ , thus the vertices of  $I_1(D_X)$  and  $I_2(D_X)$  are all the oriented coloured diagonals of  $\Pi$  crossing  $D_X$ .

If  $D_X$  is a single coloured diagonal of  $\Pi$ , we need to distinguish between the diagonals inside  $I_i(D_X)$  and  $\rho(I_i(D_X))$ ,  $i = 1, 2$ . Then we observe that the coloured oriented diagonals in  $I_1(D_X)$  and  $I_2(D_X)$  are precisely the ones satisfying the assumptions of the proposition.  $\square$

**5.3. Curves of oriented coloured diagonals.** The aim of this section is to divide the Ext-hammocks in  $\mathcal{C}_{E_6}$  into curves. The reason why we do this is because for each coloured oriented diagonal  $D_X$  we want to find a uniform geometric description of the elements inside the Ext-hammock of  $D_X$ . Since the hammocks in  $\mathcal{C}_{E_6}$  are very big, this goal seems hopeless. However, dividing the Ext-hammock of  $D_X$  into smaller sets, allows us to describe the elements of each such set in geometric terms. We will call these sets curves.

Let  $X$  be an indecomposable object of  $\mathcal{C}_{E_6}$  and let  $D_X$  be the corresponding coloured oriented diagonal viewed as a vertex of  $\Gamma$ . For  $r \in \{2, 4\}$ , the curves  $C_1(D_X), \dots, C_r(D_X)$  of  $D_X$  in  $\Gamma$  are  $r$  collections of oriented coloured diagonals having non-vanishing extensions with  $D_X$ . Each collection  $C_i(D_X)$  has the shape of a curve in  $\Gamma$ .

We begin defining the curves of  $D_X$ , for  $D_X$  in the first slice of  $\Gamma$ . For all other vertices  $D_X$  of  $\Gamma$ , curves can be defined from the previous ones by  $\tau$ -shifts. The first curve of  $[1, 6]_R$ , denoted by  $C_1([1, 6]_R)$ , is defined as follows:

$$\begin{aligned} C_1([1, 6]_R) := & \{[7, 2+i]_c, 0 \leq i \leq 3, c \in \{R, P\}\} \\ & \cup \{[5, 7+i]_c, 0 \leq i \leq 3, c \in \{R, P\}\} \\ & \cup \{[6, 3]_R\}. \end{aligned}$$

The second curve of  $[1, 6]_R$ , denoted by  $C_2([1, 6]_R)$ , is defined as follows:

$$\begin{aligned} C_2([1, 6]_R) := & \{[5-i, 7]_c, 0 \leq i \leq 3, c \in \{B, P\}\} \\ & \cup \{[2, 7+i]_c, 0 \leq i \leq 3, c \in \{B, P\}\} \\ & \cup \{[1, 4]_B\}. \end{aligned}$$

By definition  $C_1([1, 6]_R)$  is obtained by the sequence of minimal clockwise rotations around the vertices 7, 5, 3 of  $\Pi$  starting in  $\tau^{-1}([1, 6]_R) = [2, 7]_R$  and ending with  $[6, 3]_R$ . Dually,  $C_2([1, 6]_R)$  is obtained by a sequence of minimal anticlockwise rotations around the vertices 7, 2, 4 starting in  $\tau([1, 6]_R) = [5, 7]_B$  and ending in  $[1, 4]_B$ .

By construction the Ext-hammock of  $[1, 6]_R$  is  $C_1([1, 6]_R) \cup C_2([1, 6]_R)$ . In Figure 8(a) the elements of  $C_1([1, 6]_R)$  are drawn in the upper half of  $\Gamma$ , while the elements of  $C_2([1, 6]_R)$  are in the lower half.

Next, we are going to associate four curves to  $[1, 5]_R$ . The first curve of  $[1, 5]_R$ ,  $C_1([1, 5]_R)$ , is the set containing coloured oriented diagonals of  $\Pi$  obtained by a sequence of minimal clockwise rotations around the vertices 6, 4, 2 starting in  $\tau^{-1}([1, 5]_R)$  and ending in  $[5, 2]_R$ . The third curve  $C_3([1, 5]_R)$  is obtained by a sequence of minimal anticlockwise rotations around the vertices 7, 2, 4 starting with  $\tau([1, 5]_R)$  and ending in  $[1, 4]_B$ . Moreover,  $C_2([1, 5]_R)$  coincides with  $C_1([1, 6]_R)$ , and  $C_4([1, 5]_R)$  coincides with  $C_2([1, 6]_R)$ .

For  $D_X \in \{[1, 6]_R, [1, 5]_R\}$ , the curves of  $C_1(\rho(D_X)), \dots, C_r(\rho(D_X))$  of  $\rho(D_X)$  are defined by  $\rho(C_1(D_X)), \dots, \rho(C_r(D_X))$ ,  $r \in \{2, 4\}$ .

We are left with defining the curves of the paired diagonals  $[1, 3]_P$  and  $[1, 4]_P$ . For  $[1, 3]_P$  we have  $C_1([1, 3]_P)$  given by the set containing both single and paired coloured oriented diagonals obtained by a sequence of minimal rotations in the clockwise order around the vertices 2, 7, 5 starting in  $\tau^{-1}([1, 3]_P)$  and ending in  $[5, 1]_P$ . Similarly  $C_2([1, 3]_P)$  is obtained by a sequence of minimal anticlockwise rotations around the vertices 2, 4, 5 starting in  $\tau([1, 3]_P)$  and ending in  $[6, 2]_P$ .

Next,  $C_1([1, 4]_P)$  is obtained by a sequence of minimal clockwise rotations starting in  $\tau^{-1}([1, 4]_P)$  and ending in  $[5, 1]_P$ .  $C_3([1, 4]_P)$  is obtained rotating in the anticlockwise order  $\tau([1, 4]_P)$  to  $[4, 7]_P$ . Finally,  $C_2([1, 4]_P) = \tau^{-1}(C_1([1, 3]_P))$  and  $C_4([1, 4]_P) = C_2([1, 3]_P)$ .

In Figure 8(a)-(f) we represent the various curves of  $D_X$ , for  $D_X$  be in the first (and last) slice of  $\Gamma$ . The numbers 1, 2, 3, 4 indicate the starting term of the curves  $C_1(D_X), \dots, C_4(D_X)$  and the colours of the heptagons indicate the curves they intersect.

#### 5.4. Intersections of curves.

**Proposition 5.3.** *Let  $D_X, D_Y$  be vertices of  $\Gamma$ . Let  $C_1(D_X), \dots, C_r(D_X)$  be the curves of  $D_X$ ,  $r \in \{2, 4\}$ . Then  $\dim_k(\text{Ext}_{\Pi}^1(D_X, D_Y))$  is equal to the number of curves of  $D_X$  intersecting with  $D_Y$  in  $\Gamma$  (0 up to 3).*

*Proof.* First, the Ext-hammocks in the AR-quiver of  $\mathcal{C}_{E_6}$  are invariant under  $\tau$ -shifts. After changing the image of the projective objects of  $\text{mod}kE_6$  in the equivalence of Theorem 4.3 we can assume that  $X$  or  $Y$  corresponds to a diagonal in the first slice of  $\Gamma$ . By remark 5.1 we can treat the cases where  $D_X$ , or  $D_Y$  belongs to the first slice of  $\Gamma$  in the same way. Second, the curves of  $D_X$  are by construction such that their intersection points coincide with the vertices  $D_Y$  in  $\Gamma$  for which  $\dim_k(\text{Ext}_{\Pi}^1(D_X, D_Y)) \geq 1$ . From the definition of morphisms in the

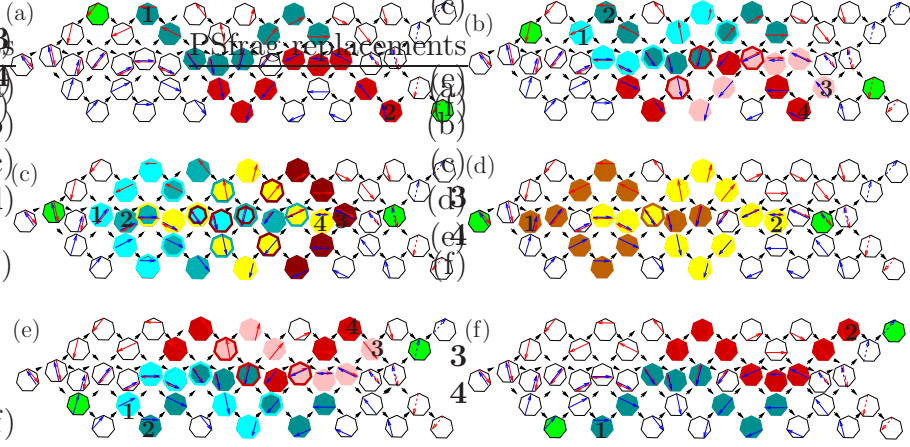


FIGURE 8. Decomposition into curves of the Ext-hammocks of the vertices in the first slice of  $\Gamma$ .

mesh category of a stable translation quiver, it follows that the number of curves intersecting in  $D_Y$  is the dimension of  $\text{Ext}_{\mathcal{C}_{E_6}}^1(D_X, D_Y)$ .  $\square$

Let again  $D_X$  be in the first slice of  $\Gamma$ . In Figure 8(a)-(f) the dimension of the space  $\dim_k(\text{Ext}_{\Pi}^1(D_X, D_Y))$  is expressed by the numbers of colours filling the heptagon containing  $D_Y$ . If  $D_Y$  is in a white heptagon of  $\Gamma$  then  $\dim_k(\text{Ext}_{\Pi}^1(D_X, D_Y)) = 0$ .

More precisely, the two curves represented in Figure 8(a) and (f) never intersect, and  $\dim_k(\text{Ext}_{\Pi}^1(D_X, D_Y)) = 1$  for  $D_Y$  in a coloured heptagon, and  $D_X$  in the first slice of  $\Gamma$ .

In Figure 8(b) and (e) the curve  $C_1(D_X)$  intersects  $C_2(D_X)$  in two vertices. Similarly, for  $C_3(D_X)$  and  $C_4(D_X)$ . The curve  $C_2(D_X)$  intersects  $C_4(D_X)$  only once. The five heptagons where two curves meet have two colours (boundary and interior of the heptagon). Then  $\dim_k(\text{Ext}_{\Pi}(D_X, D_Y)) = 2$  for  $D_Y$  corresponding to one of these heptagons.

In Figure 8(c) there are two heptagons where three curves meet. They are drawn with three colours, and hence  $\dim_k(\text{Ext}_{\Pi}(D_X, D_Y)) = 3$  for  $D_Y$  corresponding to one of these two. Moreover, in nine heptagons two curves meet, and they are drawn in two colours.

Finally, in Figure 8(d) two curves are drawn, and they intersect only in one vertex of  $\Gamma$ .

**5.5. Cluster tilting objects.** Let  $Q$  be an orientation of a simply-laced Dynkin graph with  $n$  vertices. Let  $\mathcal{T} = \{T_1, T_2, \dots, T_n\}$  be a set of pairwise non isomorphic indecomposable objects of  $\mathcal{C}_Q$ . If  $\text{Ext}_{\mathcal{C}_Q}^1(T_i, T_j) = 0$  for all  $T_i, T_j \in \mathcal{T}$ , then one says that  $\mathcal{T}$  is a *cluster tilting set* of  $\mathcal{C}_Q$ .

A *cluster tilting object* in  $\mathcal{C}_Q$  is the direct sum of all objects of a cluster tilting set in  $\mathcal{C}_Q$ . Observe that knowing a cluster tilting objects allows to determines a cluster tilting set and viceversa. Moreover, given a cluster tilting set  $\mathcal{T}$ , one says that  $\overline{T} = \bigoplus_{j \neq i} T_j$ ,  $T_j \in \mathcal{T}$  is an *almost complete cluster tilting object* if there is an indecomposable object  $T_i^*$  in  $\mathcal{C}_Q$  such that  $\overline{T} \oplus T_i^*$  is a cluster tilting object of  $\mathcal{C}_Q$ . The object  $T_i^*$  is called the *complement* of  $T_i$ .

The *mutation at  $i$*  of a cluster tilting object  $\mathcal{T}$  in  $\mathcal{C}_Q$ , for  $1 \leq i \leq n$ , is the operation which replaces the indecomposable summand  $T_i$  in  $\bigoplus_{j=1}^n T_j$  with the complement  $T_i^*$  of  $T_i$  in  $\overline{T} = \bigoplus_{j \neq i} T_j$ .

The statements in the next Theorem are shown in [3].

**Theorem 5.4.** *Let  $T$  be a cluster tilting object in  $\mathcal{C}_Q$ .*

- *each almost complete cluster tilting object  $\overline{T}$  in  $\mathcal{C}_Q$  has exactly two complements,  $T$  and  $T^*$ .*
- *If  $T$  and  $T^*$  are complements of  $\overline{T}$  then  $\dim_k(\text{Ext}_{\mathcal{C}_Q}^1(T, T^*)) = 1$ . On the other side, if  $\dim_k(\text{Ext}_{\mathcal{C}_Q}^1(T, T^*)) = 1$ , then there is an almost complete cluster tilting object  $\overline{T}$  such that  $T$  and  $T^*$  are complements of  $\overline{T}$ .*

After Proposition 3.8 in [9] and [3, Thm. 4.5] we know that there are 833 cluster tilting sets, hence cluster tilting objects, in  $\mathcal{C}_{E_6}$ .

From the work of Caldero-Chapoton-Schiffler, see [5], we know that cluster tilting objects of  $\mathcal{C}_{A_n}$  are in bijection with the formal direct sums of diagonals belonging to a maximal collection of non-crossing diagonals in a regular  $(n+3)$ -gon. In this context mutations corresponds to *flips* of diagonals. More precisely, a flip replaces a diagonal  $D_i$  in a given triangulation  $\Delta$  with the unique other diagonal  $D_i^*$  crossing  $D_i$  and completing  $\Delta \setminus D_i$  to a new triangulation of the regular  $(n+3)$ -gon.

## 5.6. First fundamental family of cluster configurations of $\Pi$ .

Our next aim is to describe cluster tilting sets of  $\mathcal{C}_{E_6}$  as configurations of single and paired coloured oriented diagonals in  $\Pi$ .

**Definition 5.5.** *A cluster configuration is a family of pairwise different coloured oriented diagonals of  $\Pi$ ,  $\mathcal{T} = \{D_1, D_2, \dots, D_6\}$ , with the property that  $\text{Ext}_{\Pi}^1(D_i, D_j) = 0$  for all  $D_i, D_j \in \mathcal{T}$ . A coloured oriented diagonal  $D_i^*$  is called complement of  $D_i$  in  $\mathcal{T}$  if  $D_i^* \neq D_i$  and  $\mathcal{T}'$  obtained from  $\mathcal{T}$  after replacing  $D_i$  by  $D_i^*$  is a cluster configuration of  $\Pi$ .*

Consider two heptagons, and a long paired diagonal  $L_P := [i, i+3]_P$ ,  $i \in \mathbb{Z}/7\mathbb{Z}$  of  $\Pi$ . Our next goal is to complete  $L_P$  to a set of coloured oriented diagonals inside the two heptagons, giving rise to a cluster

configuration of  $\Pi$ . For this we remark that  $L_P$  divides each  $\Pi$  into the quadrilateral  $\Pi_4$  with boundary vertices  $\{i, i+1, i+2, i+3\}$ , and the pentagon  $\Pi_5$  with boundary vertices  $\{i, i+3, i+4, i+5, i+6\}$ ,  $i \in \mathbb{Z}/7\mathbb{Z}$ .

In Lemma 5.6 below we will see that triangulating  $\Pi_4$  with a short paired diagonal, and each  $\Pi_5$  with single diagonals of the appropriate colour gives rise to cluster configurations.

**Lemma 5.6.** *Let  $L_P := [i, i+3]_P$ ,  $i \in \mathbb{Z}/7\mathbb{Z}$ .*

- *For  $i \neq 1$ , triangulating each  $\Pi_5$  with single diagonals of the same colour, and  $\Pi_4$  with a short paired diagonal gives a cluster configuration  $\mathcal{T}_{L_P}$  of  $\Pi$ .*
- *All cluster configurations of  $\Pi$  containing  $[j, j+3]_P$  arise as  $\tau^k(\mathcal{T}_{L_P})$ ,  $1 \leq j, k \leq 7$ .*

*Proof.* Since  $i \neq 1$  we can assume that the region in  $\Gamma$  outside the Ext-hammock of  $L_P$  has only blue diagonals below  $L_P$  and only red diagonals above  $L_P$ . Observe that the diagonals outside the Ext-hammock are precisely the diagonals involved in triangulations of the two copies of  $\Pi_5$  and  $\Pi_4$ .

Then choose a short paired diagonal  $S_P$  triangulating  $\Pi_4$  with a short paired diagonal. Then triangulating a copy of  $\Pi_5$  with only single red diagonals, and triangulating the second copy of  $\Pi_5$  with only single blue diagonals yields a cluster configuration. With Proposition 5.2 we deduce that the arcs obtained in this way have no extension in each region above and below  $L$  in  $\Gamma$ . One can then check that the Ext-hammocks in one region do not pass through the other region, nor through  $S_P$ . Thus, to each red triangulation one can choose a blue triangulation of  $\Pi_5$ , and all choices are possible. Similarly, one can complete  $\{L_P, S_P^*\}$  to a cluster configuration, where  $S_P^*$  is the other short paired diagonal triangulating  $\Pi_4$ . Notice that there are no other possibilities to complete  $L_P$  to a cluster configuration of  $\Pi$ . Next, there are 7 choices for  $L_P$  in  $\Gamma$ . For each choice of  $L_P$  the associated cluster configurations are obtained from the previous by rotation through  $\tau$ . Adjustment of the colours-orientations of the single diagonals triangulating  $\Pi_5$  are needed if  $L_P$  is the first slice of  $\Gamma$ .  $\square$

Notice that the two triangulations of  $\Pi_5$  can be different, and the color is uniquely determined by the position of  $L_P$  in  $\Pi$ , resp. in  $\Gamma$ .

In the following we call the cluster configurations given by a long paired diagonal and coloured oriented single and paired diagonals triangulating two copies of  $\Pi_5$  and  $\Pi_4$ , as describe in the first part of

Lemma 5.6, the *first fundamental family* of cluster configurations. We denote this family by  $\mathcal{F}_1$ .

### 5.7. Second fundamental family of cluster configurations of $\Pi$ .

We saw in Lemma 5.6 that many cluster configurations correspond to two triangulations of  $\Pi$ . Our next goal is to define a second family of cluster configurations describing the remaining cluster tilting set of  $\mathcal{C}_{E_6}$ . For this the following general observation is needed.

For  $i \in \mathbb{Z}/7\mathbb{Z}$ , consider the long single red diagonal  $L = [i, i + 4]_R$  of  $\Pi$ . Then  $L$  divides  $\Pi$  into the quadrilateral  $\Pi_4 := \{i + 4, i + 5, i + 6, i\}$ , and the pentagon  $\Pi_5 := \{i, i + 1, i + 2, i + 3, i + 4\}$ . Let  $\mathcal{T}_L$  be a cluster configuration of  $\Pi$  containing  $L$ . Then  $\mathcal{T}_L$  necessarily also contains one of the two short single diagonals triangulating  $\Pi_4$ , neighbouring  $L$  in  $\Gamma$ . Similarly for  $\rho(L) = [i + 4, i]_B$ . More precisely,

**Lemma 5.7.** *Let  $i \in \mathbb{Z}/7\mathbb{Z}$ ,  $L = [i, i + 4]_R$  in  $\Pi$ , and  $\mathcal{T}_L$  be a cluster configuration containing  $L$ .*

- *If  $i \neq 1$ , exactly one of  $\{[i, i + 5]_R, [i + 6, i + 4]_R\}$  is in  $\mathcal{T}_L$ .*
- *If  $i = 1$ , exactly one of  $\{[i, i + 5]_R, \rho([i + 6, i + 4]_R)\}$  is in  $\mathcal{T}_L$ .*

*Similarly for  $\rho(L)$ . Moreover, in each case the two diagonals are complements to each other.*

*Proof.* Let  $i \neq 1$  and consider the Ext-hammock of  $L$  in  $\Gamma$ . Since  $L$  is not in the first slice of  $\Gamma$  the diagonals triangulating  $\Pi_4$  have the same color as  $L$ . Then one can check that all Ext-hammocks of objects outside the Ext-hammock of  $L$ , which are different from  $[i, i - 2]_R$  and  $[i - 1, i - 3]_R$ , never contain single diagonals inside the quadrilateral  $\Pi_4$  in  $\Pi$ . Thus, by maximality we deduce that all cluster tilting sets containing  $L$  necessarily also contain one of the diagonals inside  $\Pi_4$ . Taking one diagonal triangulating  $\Pi_4$  rules out the other, thus the two single diagonals triangulating  $\Pi_4$  are complements to each other. For  $i = 1$ ,  $L$  is in the first slice of  $\Gamma$ . Then one can proceed as before adjusting the colour of the diagonal triangulating  $\Pi_4$ .  $\square$

In view of the next result, we point out that the short single diagonals of Lemma 5.7, triangulating  $\Pi_4$  and neighbouring  $L$  in  $\Gamma$ , are displayed in filled light grey heptagons in Figure 9(a)-(n).

**Lemma 5.8.** *Every six-tuple of diagonals of Figure 9(a)-(n) determines a cluster configuration of  $\Pi$ .*

*Proof.* For each choice of a short single diagonal of Lemma 5.7 triangulating  $\Pi_4$  and neighbouring  $L$  in  $\Gamma$ , the claim can be verified by checking that the diagonals in the highlighted heptagons have no extension among each other.  $\square$

In the following, we refer to the collection of cluster configurations of Figure 9(a)-(n) as the *second fundamental family* of cluster configurations of  $\Pi$ , and we denote this family by  $\mathcal{F}_2$ .

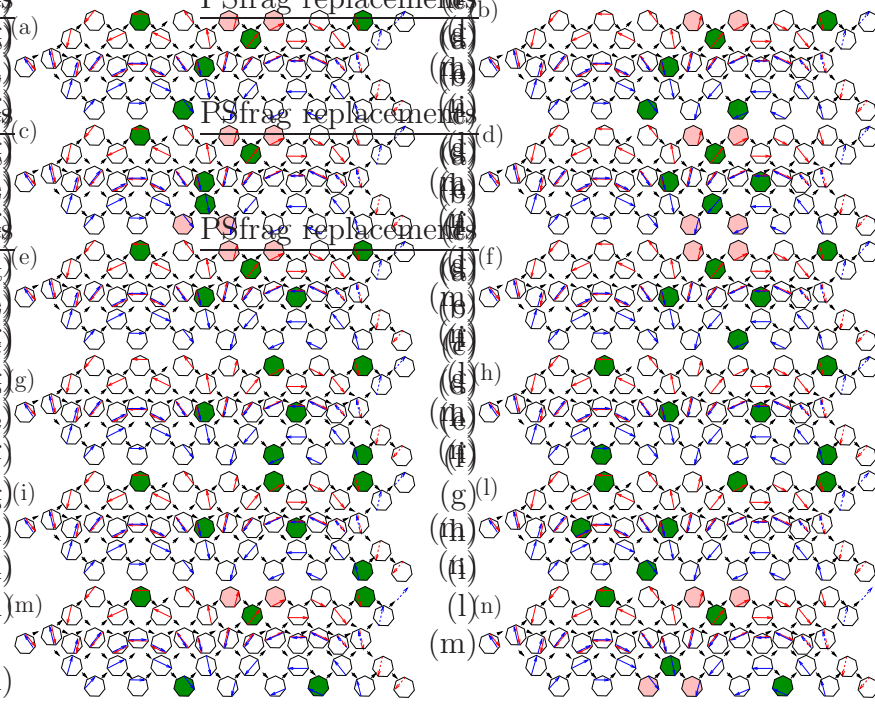


FIGURE 9. The second fundamental family of cluster configurations of  $\Pi$ .

**5.8. Symmetries in  $\Pi$  leading to cluster configurations.** We determine two symmetries in  $\Pi$  leading to cluster configurations. One symmetry simply switches colours and orientations of the coloured oriented diagonals of a given cluster configuration. The second one arises from a left-right symmetry of  $\Gamma$ , and corresponds to a reflection in  $\Pi$ .

There are two reasons why these symmetries are important. First, using these symmetries we can deduce all cluster configurations starting from the sets in  $\mathcal{F}_2$ . Second, knowing how a cluster configuration behaves under mutation, allows to understand how the symmetric ones behave.

Let  $c \in \{R, B\}$ . For  $i \in \mathbb{Z}/7\mathbb{Z}$  let  $h_i$  be the line in  $\Pi$  passing through  $i$  and the middle point of  $i+3, i+4$ . On all coloured oriented diagonals different then  $[i \pm 1, i \mp 1]_c$ , let  $\sigma_i : \Pi \rightarrow \Pi$  be the reflection in  $\Pi$  along  $h_i$  followed by a switch of orientation. Otherwise,  $\sigma_i([i \pm 1, i \mp 1]_c) := \rho([i \pm 1, i \mp 1]_c)$ .

In Figure 10 we illustrate on the left the cluster configuration (g) and on the right we show the cluster configuration obtained after applying  $\sigma_6$  to it.

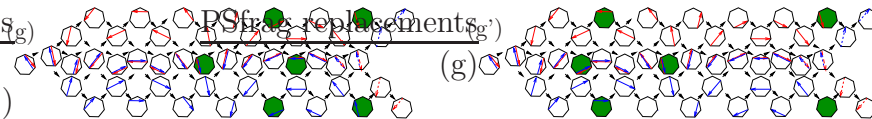


FIGURE 10.  $\sigma$ -symmetric cluster configurations of  $\Pi$ .

**Lemma 5.9.** *Let  $\mathcal{T}$  be a cluster configuration belonging to  $\mathcal{F}_2$ . Then  $\rho(\mathcal{T})$ , and  $\sigma_6(\mathcal{T})$  are also cluster configurations.*

*Proof.* Apply the map  $\rho$ , resp.  $\sigma_6$  to the cluster configuration of Lemma 5.8. Because of the shape of the Ext-hammocks one indeed produces cluster configurations.  $\square$

Notice that the set  $\rho(\mathcal{T})$  of a cluster configuration  $\mathcal{T}$  is an element of the  $\tau$ -orbit of  $\mathcal{T}$ , while  $\sigma_i(\mathcal{T})$  does not belong to any  $\tau$ -orbit of a cluster configuration of  $\mathcal{F}_2$  (nor of  $\mathcal{F}_1$ ).

**5.9. Classification of cluster tilting sets of  $\mathcal{C}_{E_6}$ .** From [9, Prop. 3.8] and [3, Thm. 4.5] we know that there are 833 cluster tilting sets in  $\mathcal{C}_{E_6}$ . In the next result we give a complete geometric classification of all cluster tilting sets in  $\mathcal{C}_{E_6}$  in terms of cluster configurations of  $\Pi$ .

**Theorem 5.10.** *In  $\Pi$*

- 350 different cluster configurations have one long paired diagonal, and they arise from  $\mathcal{F}_1$  through  $\tau$ .
- 483 other cluster configurations arise from  $\mathcal{F}_2$  through  $\sigma$  and  $\tau$ .

**Corollary 5.11.** *In  $\Pi$ :*

- 224 cluster configurations have precisely one short paired diagonal,
- 175 cluster configurations have precisely two short paired diagonals,
- 84 cluster configurations have no paired diagonals of  $\Pi$ .

*All these cluster configurations are different.*

*Proofs of Theorem 5.10 and Corollary 5.11.* The first part of the claim follows from Lemma 5.6. In fact, we saw that for each long paired diagonal  $L_p$  there are 25 ways to triangulate one of the two pentagons  $\Pi_5$  with single coloured diagonals. Moreover, there are two ways to triangulate  $\Pi_4$  with short paired diagonals. Thus, each  $L_p$  gives rise to

50 different cluster configurations. Since there are 7 choices for  $L_p$  in  $\Pi$ , the first claim follows.

For the second part of the claim the idea is to consider different cases, depending on the number of short paired diagonals leading to cluster configurations. First case: the only paired diagonal of  $\mathcal{T}$  is a short one. Then  $\mathcal{T}$  arises from the collection highlighted in (a),(b) or (c) in Figure 9, up to  $\tau$ -shifts and the  $\sigma$ -symmetry of Lemma 5.9. Moreover, after Lemma 5.7 for each coloured oriented diagonal  $[i, i-3]_c$ ,  $c \in \{R, B\}$  in  $\mathcal{T}$  there two possible choices of neighbouring short single diagonals in  $\mathcal{T}$ . Consequently, up to  $\tau$ -shifts, there are 4 different cluster configurations arising from a collection of diagonals as in (a). Similarly for (b). The collection in (c) gives rise to 8 different cluster configurations up to  $\tau$ -shifts, as there are 4 choices for short single diagonals, and further 4 arise by taking the  $\sigma$ -symmetric case.

Summing up, the cluster configurations in (a), (b), (c) give rise to 224 different cluster configurations.

Second case:  $\mathcal{T}$  has exactly two short paired diagonals. Then one distinguishes further into (d),(e) and (f) which have single coloured oriented diagonals of the form  $[i, i+3]_c$ ,  $c \in \{R, B\}$ . While the cluster configurations in (g),(i),(h) and (l) only contain short single diagonals of the form  $[i, i+2]_c$ ,  $c \in \{R, B\}$ . Proceeding as before, taking into account the symmetry  $\sigma$  of Lemma 5.9 one obtains the claimed number.

In the third case we count the cluster configurations arising from  $\tau$ -shifts of the cluster configurations in (m) and (n) having no paired diagonals. As before we deduce that there are 28 the cluster configurations arising from  $\tau$ -shifts of (m) and 56 arising from  $\tau$ -shifts of the 4 cluster configurations in (n). Together this gives 84 cluster configurations without paired diagonals.  $\square$

**5.10. The geometry of cluster configurations.** In Section 5.6 we saw that cluster configurations in  $\mathcal{F}_1$  correspond to triangulations with coloured oriented diagonals of two copies of  $\Pi$ . Cluster configurations of  $\mathcal{F}_2$  are not as simple to describe. In Theorem 5.12 below we can give a general statement concerning the geometry of cluster configurations in  $\Pi$ .

**Theorem 5.12.** *All 833 cluster tilting sets of  $\mathcal{C}_{E_6}$  can be expressed as configurations of six non-crossing coloured oriented single and paired diagonals inside two heptagons.*

*Proof.* First, given a cluster configurations in  $\mathcal{F}_1 \cup \mathcal{F}_2$  we divide the coloured oriented diagonals inside two heptagons by colour. Paired diagonals appear in both heptagons.

Then we observe that all cluster configurations in  $\mathcal{F}_1$  and  $\mathcal{F}_2$  are crossing free. Moreover, the symmetry  $\sigma$  produces new configurations of diagonals which are again crossing free. Taking  $\tau$ -shifts only rotates the entire configurations inside the two heptagons, occasionally switching colours and orientation according to the action of  $\tau$  inside  $\Pi$ . Hence the crossing free property is preserved under  $\tau$ -shifts and the claim follows.  $\square$

The cluster configuration  $\mathcal{T} = \{[5, 3]_R, [5, 2]_R, [5, 1]_P, [5, 6]_P, [3, 5]_B, [2, 5]_B\}$  is expressed in two heptagons in the center of Figure 11, the numbering of the vertices of one heptagon is highlighted in the figure. Paired diagonals appear in both heptagons and have labels.

The converse statement of Theorem 5.12 is not true, as configurations of non-crossing coloured diagonals different then cluster configurations of  $\Pi$  are not cluster tilting sets of  $\mathcal{C}_{E_6}$ .

**5.11. Mutations of cluster tilting objects in  $\mathcal{C}_{E_6}$ .** In this section we will see that in many cases it is possible to deduce the mutation process in  $\mathcal{C}_{E_6}$  from the mutations process inside  $\mathcal{C}_{A_4}$ . Moreover, we can deduce the mutation process for the families in  $\mathcal{F}_1$  and  $\mathcal{F}_2$  and taking  $\tau$ -shifts extend it for the remaining cluster configurations.

In the next definitions we indicate by  $\overline{D}$  the unoriented single diagonal corresponding to a coloured oriented diagonal  $D$  of  $\Pi$ .

**Definition 5.13.** *Let  $D_P$  be a paired oriented diagonal and let  $\mathcal{T}$  be a cluster configuration containing  $D_P$ . The paired diagonal  $D_P^*$  is the flip-complement of  $D_P$ , if  $\overline{D}_P$  and  $\overline{D}_P^*$  are related by a flip.*

**Definition 5.14.** *Let  $D_S$  be a single coloured oriented diagonal and let  $\mathcal{T}$  be a cluster configuration containing  $D_S$ . The single coloured oriented diagonal  $D_S^*$  is the flip-complement of  $D_S$  in  $\mathcal{T}$ , if  $\overline{D}_S$  and  $\overline{D}_S^*$  are related by a flip and  $\mathcal{T} \setminus D_S \cup D_S^*$  is a cluster configuration.*

Notice that if a flip-complement exists then the colour and orientation is uniquely determined by Lemma 5.6 and Lemma 5.7.

**Proposition 5.15.** *Let  $D_L$  be a long coloured oriented diagonal of  $\Pi$  giving rise to a cluster configuration.*

- *If  $D_L$  is paired: single coloured diagonals triangulating  $\Pi_5$ , and paired diagonals triangulating  $\Pi_4$  have a flip-complement.*
- *If  $D_L$  is single: single diagonals triangulating  $\Pi_4$  have a flip-complement.*

*Proof.* Let  $D_L$  be a long coloured oriented diagonal dividing  $\Pi$  into the quadrilateral  $\Pi_4$  and the pentagon  $\Pi_5$ . In Lemma 5.6 we saw that if  $D_L$

is paired, triangulating  $\Pi_4$  with a paired diagonal, and two copies of  $\Pi_5$  with single oriented diagonals, always gives a cluster configuration. Hence removing a single diagonal of a copy of  $\Pi_5$  or a paired diagonal triangulating  $\Pi_4$  can only be completed to a cluster configuration in two ways, namely with diagonals being flip-complement of each other. If  $D_L$  is single, the claim follows from Lemma 5.7.  $\square$

Further instances of the mutation process in  $\mathcal{C}_{E_6}$  can be described by flips of coloured oriented diagonals in  $\Pi$ , but not all mutations allow a description of this type. This is unsurprising, as for example not all mutations in the cluster algebra  $\mathbb{C}[Gr_{3,7}]$  can be described through Plücker relations, see [20].

With Figure 9 it is not hard to deduce all the remaining mutations occurring. For example, the cluster configuration in (a) can be mutated to (b),(c),(e),(l),(m) and to the flip of a diagonal inside one light grey coloured heptagon. Similarly, we have a list for the other families. Some instances of the more complicated geometric exchanges can be found on the upper pentagon of Figure 11.

**5.12. Exchange graph.** In Figure 11 we display a part of the *exchange graph* of  $\mathcal{C}_{E_6}$ . For each heptagon appearing in the figure the numbering of its vertices is as shown on the central heptagon. The vertices of the graph correspond to cluster configurations, hence to cluster tilting sets of  $\mathcal{C}_{E_6}$ , edges are drawn when two cluster configurations are related by a single mutation. In the two central heptagons of Figure 11 the configuration of  $\mathcal{T} = \{[5, 3]_R, [5, 2]_R, [5, 1]_P, [5, 6]_P, [3, 5]_B, [2, 5]_B\}$  is displayed. The 8 neighbouring configurations are placed on the vertices of the two central pentagons sharing the vertex corresponding to  $\mathcal{T}$ . These 8 sets are obtained from  $\mathcal{T}$  through repeated flips of single diagonals, as described in Proposition 5.15. The vertices of the left pentagon are obtained after mutating  $[6, 2]_P$  in  $\mathcal{T}$ .

**5.13. Cluster tilted algebras.** Let  $T = T_1 \oplus \cdots \oplus T_n$  be a cluster tilting object of  $\mathcal{C}_Q$ , then  $\text{End}_{\mathcal{C}_Q}(T)$  is the *cluster tilted algebra* of type  $Q$ . The quiver  $Q_T$  of  $\text{End}_{\mathcal{C}_Q}(T)$  has no loops nor 2-cycles and it encodes precisely the exchange matrix of the cluster associated to  $T$ , see [4] and [6]. In  $\mathcal{C}_{A_n}$  the quiver  $Q_T$  can be read off from the triangulation  $T$ , see [5]. The vertices of  $Q_T$  are the diagonals of the triangulation and an arrow between  $D_i$  and  $D_j$  is drawn, whenever  $D_i$  and  $D_j$  bound a common triangle. The orientation of the arrow is  $D_i \rightarrow D_j$ , if  $D_j$  is linked to  $D_i$  by an anticlockwise rotation around the common vertex.

Extending the definition of  $Q_T$  to the case at hand, the quivers corresponding to the cluster tilting sets of Figure 11 can be deduced. One

could also read off the quivers, and relations, directly from  $\Gamma$  by determining the spaces  $\text{Hom}_{\mathcal{C}_{E_6}}(T, T)$ .

## 6. APPLICATIONS AND FURTHER DIRECTIONS

**6.1. Symmetric cluster configurations and the cluster algebra of type  $F_4$ .** Cluster categories arising from valued quivers have been first categorified algebraically in [7]. The aim of this section is to use the geometric description of the cluster category  $\mathcal{C}_{E_6}$  to categorify geometrically the cluster algebra of type  $F_4$ .

Consider again the map  $\rho$  given by a simultaneous change of colour and orientation of coloured oriented diagonals of  $\Pi$ .

**Definition 6.1.** *A cluster configuration  $\mathcal{T}$  in  $\Pi$  is  $\rho$ -symmetric if  $\mathcal{T} = \rho(\mathcal{T})$ .*

Since we know all cluster configurations of  $\Pi$ , see Theorem 5.10, we can deduce that there are only three types of  $\rho$ -symmetric cluster configurations in  $\Pi$ . First, cluster configurations of  $\Pi$  projecting to triangulations of  $\Pi$  consisting of unoriented arcs through  $\mathcal{C}_{E_6} \rightarrow \mathcal{C}_{A_4}$ . These arise from  $\mathcal{F}_1$  and from  $\tau$ -shifts of the configurations in Figure 9(d). Second,  $\tau$ -shifts of both, the cluster configuration in Figure 9(g) and the  $\sigma$ -symmetric configuration of Figure 9(g'). Third,  $\tau$ -shifts of the configuration in Figure 9(h). We call the first  $\rho$ -symmetric cluster configurations of type **T**, the second of type **C** and the third of type **L**. Moreover, we refer to the double short diagonals in a configuration of type **C** as middle diagonals.

In Figure 12 configurations of type **L** and **C** are illustrated. The blue diagonals have opposite orientation with respect to the ones shown in the figure and are omitted. The two  $\rho$ -symmetric cluster configurations of type **C** on the right side of the figure are related through the action of  $\sigma_6$ , already defined in Section 5.8. Notice that for  $\rho$ -symmetric cluster configurations the quiver  $Q_T$  of  $\text{End}_{\mathcal{C}_{E_6}}(T)$  is symmetric.

In the next result we show that mutations of cluster tilting objects in  $\mathcal{C}_{E_6}$  preserves the  $\rho$ -symmetry of the cluster configuration.

Let  $\mathcal{T}_\rho$  be a  $\rho$ -symmetric cluster configuration of  $\Pi$  and denote by  $D^*$  the unique complement in  $\mathcal{C}_{E_6}$  of  $D$  in  $\mathcal{T}_\rho$ . Then we observe that  $\rho$ -symmetric cluster configurations always have two  $\rho$ -orbits consisting of paired diagonals and two consist of single diagonals of opposite colour and orientation, thus we can assume  $\mathcal{T}_\rho := \{D_{P_1}, D_{P_2}, D_{S_1}, \rho(D_{S_1}), D_{S_2}, \rho(D_{S_2})\}$ . Keeping the notation as above, we have the following result.

**Proposition 6.2.** *Let  $1 \leq k, l \leq 2$ , then*

$$\mathcal{T}_\rho \setminus D_{P_k} \cup D_{P_k}^* \text{ and } \mathcal{T}_\rho \setminus \{D_{S_l}, \rho(D_{S_l})\} \cup \{D_{S_l}^*, \rho(D_{S_l}^*)\}$$

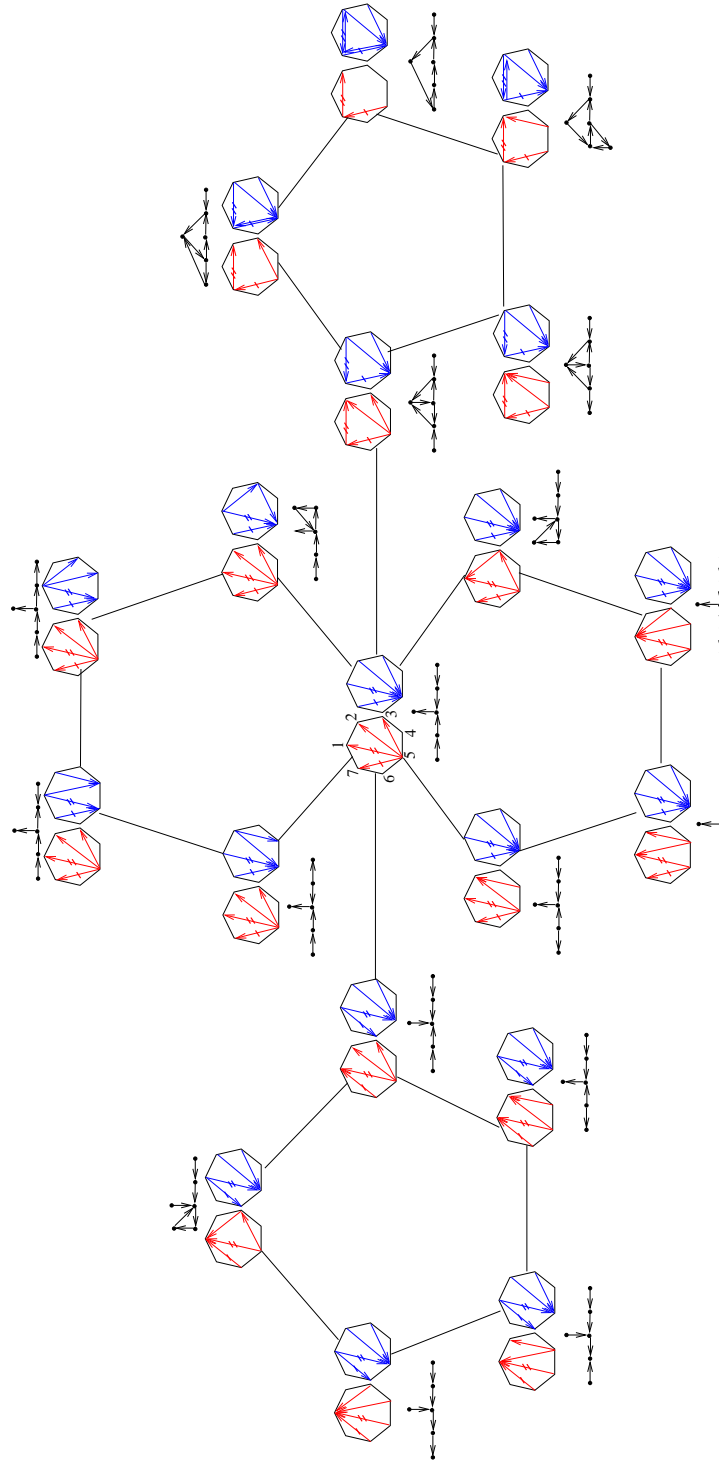


FIGURE 11. Part of the exchange graph for a cluster category of type  $E_6$ . At each vertex of the graph, the diagonals with the same labels are identified.

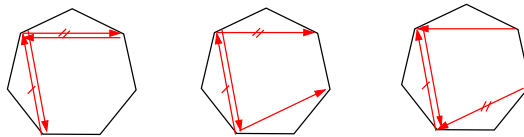


FIGURE 12.  $\rho$ -symmetric cluster configurations of type **L** and **C**.

are  $\rho$ -symmetric cluster configurations of  $\Pi$ .

*Proof.* The claim follows from the mutation rule of  $\mathcal{C}_{E_6}$  and the symmetry of the configurations. Moreover, since there are always two paired diagonals and two  $\rho$ -orbits of single diagonals in  $\mathcal{T}_\rho$  we deduce that paired diagonals are exchanged with paired diagonals, and single diagonals with single diagonals.  $\square$

We call the  $\rho$ -symmetric cluster configuration obtained from  $\mathcal{T}_\rho$  of Proposition 6.2 the *mutation of  $\mathcal{T}_\rho$  at  $D_{P_k}$ , resp. at  $\{D_{S_l}, \rho(D_{S_l})\}$* ,  $1 \leq k, l \leq 2$ . We refer to it by  $\mathcal{T}_\rho^*$ .

Let  $\mathcal{A}_{F_4}$  be the cluster algebra associated to a root system of type  $F_4$ . Then we are able to prove the claimed result.

**Proposition 6.3.** *There is a bijection*

$$\{\rho\text{-symmetric cluster configurations in } \Pi\} \rightarrow \{\text{clusters in } \mathcal{A}_{F_4}\}$$

*compatible with mutations.*

*Proof.* Clearly there is a bijection between the  $\rho$ -orbits of coloured oriented diagonals in  $\Gamma$  and the 24 cluster variables of  $\mathcal{A}_{F_4}$ .

Proceeding as in the proof of Theorem 5.10 we deduce that there are 105  $\rho$ -symmetric cluster configurations in  $\Pi$ : 84 are of type **T**, 14 of type **C** and 7 of type **L**. From [9, Prop. 3.8] we know that this number coincides with the number of clusters in the cluster algebra of type  $F_4$ ,  $\mathcal{A}_{F_4}$ .

In addition, the mutation rule in  $\mathcal{C}_{E_6}$  induces a unique mutation rule for  $\rho$ -symmetric cluster configurations of  $\Pi$ . This can simply be seen performing the mutation case by case. The mutation in  $\mathcal{C}_{E_6}$  on  $\rho$ -symmetric cluster configurations then agrees with the mutation of the cluster algebra  $\mathcal{A}_{F_4}$ , since the exchange graph associated to  $\mathcal{A}_{F_4}$  is regular of degree 4, see [9, Thm 1.15]. Thus there is essentially just one possible mutation.  $\square$

The 84  $\rho$ -symmetric cluster configurations of type **T** in  $\mathcal{C}_{E_6}$  are in 2:1 correspondence with the triangulations of  $\Pi$ , thus with the cluster tilting sets of the cluster category of type  $\mathcal{C}_{A_4}$ .

Geometrically the mutations of  $\rho$ -symmetric cluster configurations in  $\Pi$  are described by the following three moves. Let  $c \in \{R, B\}$  and let  $i$  a vertex of  $\Pi$ . We call a triangle bounded by coloured oriented diagonals in  $\Pi$  *internal* if all its edges are different then boundary edges.

**L-C:** In a configuration of type **L** the diagonals  $\{[i+3, i+1]_c, \rho([i+3, i+1]_c)\}$  exchange with  $\{[i-1, i-3]_c, \rho([i-1, i-3]_c)\}$  in a configuration of type **C**. Similarly  $[i+1, i+3]_P \leftrightarrow [i-3, i-1]_P$ .

**C-T:** In a configuration of type **C** the middle diagonals  $\{[i+2, i]_c, \rho([i+2, i]_c)\}$  exchange with  $\{[i, i-3]_c, \rho([i, i-3]_c)\}$  bounding an internal triangle in a configuration of type **T**. Similarly  $[i-2, i]_P \leftrightarrow [i, i+3]_P$ .

**T-T:** All diagonals in a configuration of type **T** not bounding an internal triangle, are exchanged with the usual flip rule. The orientation of the new diagonal is uniquely determined by the type of diagonal one exchanges. More precisely, the orientation is such that paired diagonals are exchanges with paired diagonals, and single with single.



FIGURE 13. Mutations of  $\rho$ -symmetric cluster tilting configurations.

In Figure 13 we illustrate a mutation between a  $\rho$ -symmetric cluster configuration of type **L** and of type **C**, as well as a mutation between a configuration of type **C** and type **T**. The diagonals in dotted lines are complements of each other and as before, paired diagonals are labelled.

**6.2. Cluster tilting sets in  $\mathcal{C}_{T_{r,s,t}}$ .** The construction of  $\Gamma_{r,s,t}^+$  and  $\Gamma_{r,s,t}^-$  of Section 3.4 was motivated by the following idea: glue two copies of the AR-quiver of  $\mathcal{C}_{A_{r+t+1}}^2$  along two disjoint  $\tau$ -orbits. This resulted in pairing diagonals (as in Section 3.1). In this context one can ask.

**Problem 6.4.** *How do categorical properties of the original category behave under this gluing operation? How do cluster tilting sets behave under this operation?*

The cluster categories  $\mathcal{C}_{E_7}$  and  $\mathcal{C}_{E_7}$  have finitely many cluster tilting set and they can be described as cluster configurations of coloured oriented single and paired diagonals inside a 10-gon, resp. a 16-gon,

in a similar way as we did in Section 5.9. From these configurations we can identify again a family (denoted by  $\mathcal{F}_1$  previously) of cluster configurations giving rise to triangulations of regions homotopic to a heptagon and a octagon, resp. a heptagon and a nonagon, compare with Section 5.6 and Lemma 5.6. In Figure 14 a cluster tilting set of  $\mathcal{C}_{E_7}$  arising from a projection of the projective modules in  $\text{mod } kE_7$  is represented. Similarly, in Figure 15 a cluster tilting set of  $\mathcal{C}_{E_8}$  is represented.

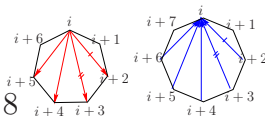


FIGURE 14. A cluster tilting set of  $\mathcal{C}_{E_7}$ .

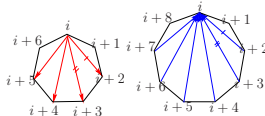


FIGURE 15. A cluster tilting set of  $\mathcal{C}_{E_8}$ .

When  $T_{r,s,t}$  is not of Dynkin type,  $\mathcal{C}_{T_{r,s,t}}$  has infinitely many cluster tilting sets. With our geometric approach, a number of cluster tilting sets of  $\mathcal{C}_{T_{r,s,t}}$  can be expressed as configurations of coloured oriented single and paired diagonals inside the  $(n+3)$ -gon  $\Pi$ , where  $n \geq \max\{r+t+1, r+s+1\}$ . Moreover, if one considers the projections  $\mathbb{Z}T_{r,s,t} \rightarrow \mathbb{Z}A_{r+t+1}$  and  $\mathbb{Z}T_{r,s,t} \rightarrow \mathbb{Z}A_{s+t+1}$  one can describe the Ext-hammocks in  $\mathbb{Z}T_{r,s,t}$  using the Ext-hammocks in  $\mathbb{Z}A_{r+t+1}$ , resp.  $\mathbb{Z}A_{s+t+1}$ , as we did in Subsection 5.2. This enable us to express a number of cluster configurations of  $\mathcal{C}_{T_{r,s,t}}$  as triangulations of a  $(s+t+4)$ - and a  $(r+t+4)$ -gon.

Finally, since in type  $A$  all quivers obtained through Fomin-Zelevinsky quiver mutations are known, we expect that our model can be used to understand the quivers in the mutation class of an orientation of  $T_{r,s,t}$ , as well as parts of the exchange graph of  $\mathcal{C}_{T_{r,s,t}}$ .

**6.3. Almost positive roots.** Consider the set of almost positive roots associated to a root system  $\Phi$ . This set, denoted by  $\Phi_{\geq -1}$ , consists of all positive roots together with all negative simple roots of  $\Phi$ .

For an initial choice of a triangulation of a regular  $(t+3)$ -gon, an explicit bijection between all (unoriented) diagonals of the polygon and the set  $\Phi_{\geq -1}$  of type  $A_t$  was given in [5].

From Theorem 4.3, together with [3, Prop. 4.1] it follows that there is a bijection between the vertices of  $\Gamma_{r,s,t}^{\pm}$  and the set of almost positive roots  $\Phi_{\geq -1}$  of the root system of type  $E_6$ ,  $E_7$  and  $E_8$ .

**Problem 6.5.** *Describe geometrically the bijection between the coloured oriented single and paired diagonals in a 7-, 10-, resp. 16-gon and the almost positive roots of the root system of type  $E_6$ ,  $E_7$ , resp.  $E_8$ .*

**Acknowledgments:** I would like to thank Karin Baur, Giovanni Felder and Robert Marsh for all the inspiring discussions we had and for the many very helpful comments. I would also like to thank an anonymous referee for helpful suggestions.

The author was partially supported by the Swiss National Science Foundation Grant Number PDFMP2127430.

#### REFERENCES

- [1] K. BONGARTZ, *Critical simply connected algebras*, Manuscripta Math., 46 (1984), pp. 117–136.
- [2] T. BRÜSTLE AND J. ZHANG, *On the cluster category of a marked surface without punctures*, Algebra Number Theory, 5 (2011), pp. 529–566.
- [3] A. B. BUAN, R. MARSH, M. REINEKE, I. REITEN, AND G. TODOROV, *Tilting theory and cluster combinatorics*, Adv. Math., 204 (2006), pp. 572–618.
- [4] A. B. BUAN, R. J. MARSH, AND I. REITEN, *Cluster mutation via quiver representations*, Comment. Math. Helv., 83 (2008), pp. 143–177.
- [5] P. CALDERO, F. CHAPOTON, AND R. SCHIFFLER, *Quivers with relations arising from clusters ( $A_n$  case)*, Trans. Amer. Math. Soc., 358 (2006), pp. 1347–1364.
- [6] P. CALDERO AND B. KELLER, *From triangulated categories to cluster algebras*, Invent. Math., 172 (2008), pp. 169–211.
- [7] L. DEMONET, *Categorification of skew-symmetrizable cluster algebras*, Algebr. Represent. Theory 14, 6 (2011), 1087–1162.
- [8] S. FOMIN AND P. PYLYAVSKYY, *Tensor graphs and cluster algebras*, arXiv:1210.1888 (2012).
- [9] S. FOMIN AND A. ZELEVINSKY, *Y-systems and generalized associahedra*, Ann. of Math. (2), 158 (2003), pp. 977–1018.
- [10] D. HAPPEL, *On the derived category of a finite-dimensional algebra*, Comment. Math. Helv., 62 (1987), pp. 339–389.
- [11] ———, *Triangulated categories in the representation theory of finite-dimensional algebras*, vol. 119 of London Mathematical Society Lecture Note Series, Cambridge University Press, Cambridge, 1988.
- [12] Peter Jørgensen. *Quotients of cluster categories*. Proc. Roy. Soc. Edinburgh Sect. A, 140(1):65–81, 2010.
- [13] B. KELLER, *On triangulated orbit categories*, Doc. Math., 10 (2005), pp. 551–581.

- [14] ———, *Cluster algebras, quiver representations and triangulated categories*, in *Triangulated categories*, vol. 375 of London Math. Soc. Lecture Note Ser., Cambridge Univ. Press, Cambridge, 2010, pp. 76–160.
- [15] L. LAMBERTI, *Repetitive higher cluster categories of type  $A_n$* , *J. Algebra Appl.* 13 (2014), no. 2, 1350091, 21 pp.
- [16] ———, *A geometric interpretation of the triangulated structure of  $m$ -cluster categories*, *Communications in Algebra*, Volume 42, Issue 3, March 2014, pages 962-983.
- [17] J.-I. MIYACHI AND A. YEKUTIELI, *Derived Picard groups of finite-dimensional hereditary algebras*, *Compositio Math.*, 129 (2001), pp. 341–368.
- [18] C. RIEDTMANN, *Algebren, Darstellungsköcher, Überlagerungen und zurück*, *Comment. Math. Helv.*, 55 (1980), pp. 199–224.
- [19] R. SCHIFFLER, *A geometric model for cluster categories of type  $D_n$* , *J. Algebraic Combin.*, 27 (2008), pp. 1–21.
- [20] J. S. SCOTT, *Grassmannians and cluster algebras*, *Proc. London Math. Soc.* (3), 92 (2006), pp. 345–380.
- [21] H. A. TORKILDSEN, *A geometric realization of the  $m$ -cluster category of type  $\tilde{A}$* , arXiv:1208.2138 (2012).
- [22] B. ZHU, *Cluster-tilted algebras and their intermediate coverings*, *Comm. Algebra*, 39 (2011), pp. 2437–2448.

MATHEMATICAL INSTITUTE, UNIVERSITY OF OXFORD, OXFORD, OX2 6GG,  
UNITED KINGDOM

*E-mail address:* Lisa.Lamberti@maths.ox.ac.uk